Published in final edited form as:
Dev Biol. 2005 June 15; 282(2): 550–570.

Gli function is essential for motor neuron induction in zebrafish

Gary Vanderlaan[a,b], **Oksana V. Tyurina**[e,1], **Rolf O. Karlstrom**[e], and **Anand Chandrasekhar**[a,b,c,d,*]

a *Division of Biological Sciences, University of Missouri, Columbia, MO 65211, USA*

b *Molecular Biology Program, University of Missouri, Columbia, MO 65211, USA*

c *Interdisciplinary Neuroscience Program, University of Missouri, Columbia, MO 65211, USA*

d *Genetics Area Program, University of Missouri, Columbia, MO 65211, USA*

e *Department of Biology, University of Massachusetts, Amherst, MA 01003, USA*

Abstract

The Gli family of zinc-finger transcription factors mediates Hedgehog (Hh) signaling in all vertebrates. However, their roles in ventral neural tube patterning, in particular motor neuron induction, appear to have diverged across species. For instance, cranial motor neurons are essentially lost in zebrafish *detour* (*gli1*$^{-}$) mutants, whereas motor neuron development is unaffected in mouse single *gli* and some double *gli* knockouts. Interestingly, the expression of some Hh-regulated genes (*ptc1*, *net1a*, *gli1*) is mostly unaffected in the *detour* mutant hindbrain, suggesting that other Gli transcriptional activators may be involved. To better define the roles of the zebrafish *gli* genes in motor neuron induction and in Hh-regulated gene expression, we examined these processes in *you-too* (*yot*) mutants, which encode dominant repressor forms of Gli2 (Gli2^{DR}), and following morpholino-mediated knockdown of *gli1*, *gli2*, and *gli3* function. Motor neuron induction at all axial levels was reduced in *yot* (*gli2*^{DR}) mutant embryos. In addition, Hh target gene expression at all axial levels except in rhombomere 4 was also reduced, suggesting an interference with the function of other Glis. Indeed, morpholino-mediated knockdown of Gli2^{DR} protein in *yot* mutants led to a suppression of the defective motor neuron phenotype. However, *gli2* knockdown in wild-type embryos generated no discernable motor neuron phenotype, while *gli3* knockdown reduced motor neuron induction in the hindbrain and spinal cord. Significantly, *gli2* or *gli3* knockdown in *detour* (*gli1*$^{-}$) mutants revealed roles for Gli2 and Gli3 activator functions in *ptc1* expression and spinal motor neuron induction. Similarly, *gli1* or *gli3* knockdown in *yot* (*gli2*^{DR}) mutants resulted in severe or complete loss of motor neurons, and of *ptc1* and *net1a* expression, in the hindbrain and spinal cord. In addition, *gli1* expression was greatly reduced in *yot* mutants following *gli3*, but not *gli1*, knockdown, suggesting that Gli3 activator function is specifically required for *gli1* expression. These observations demonstrate that Gli activator function (encoded by *gli1*, *gli2*, and *gli3*) is essential for motor neuron induction and Hh-regulated gene expression in zebrafish.

Keywords

Zebrafish; Hindbrain; Motor neuron; Induction; Rhombomere; Green fluorescent protein; Gli; Transcription factor; Hedgehog; Morpholino

* Corresponding author. Division of Biological Sciences, Room 205 Lefevre Hall, University of Missouri, Columbia, MO 65211, USA. Fax: +1 573 884 5020. *E-mail address:* AnandC@missouri.edu (A. Chandrasekhar).
[1]Present address: Department of Medicine, University of California at San Diego, La Jolla, CA 92093, USA.

Introduction

The signaling pathway initiated by the hedgehog (Hh) family of secreted proteins plays an essential role in the induction and patterning of numerous cell types during invertebrate and vertebrate development (Ingham and McMahon, 2001). Furthermore, defective Hh signaling has been implicated in tumorigenesis in humans (Wechsler-Reya and Scott, 2001), leading to extensive interest in elucidating the molecular mechanisms underlying Hh-mediated signal transduction. The Hh protein binds to a twelve-pass transmembrane protein Patched, relieving inhibition of a seven-pass transmembrane protein Smoothened and resulting in signaling into the cell. The ultimate transcriptional effectors of Hh signaling within the responding cell are the Gli family of zinc finger transcription factors (reviewed in Lum and Beachy, 2004), although Gli-independent mechanisms have also been described (Krishnan et al., 1997). Glis generally contain an N-terminal repressor domain, a zinc finger DNA-binding domain, and a C-terminal activator domain. The Drosophila *gli* homolog, *cubitus interruptus* (*ci*), is the best-understood member of this family. In the absence of an Hh signal, Ci is proteolytically cleaved between the zinc finger and the activator domains to generate a repressor that blocks expression of Hh target genes. Upon Hh binding, proteolysis of Ci is inhibited, and the full-length protein functions as a transcriptional activator of Hh target genes (Aza-Blanc et al., 1997; reviewed in Lum and Beachy, 2004). The situation in vertebrates is considerably more complex because the function of *ci* has been expanded and distributed between at least three *Gli* genes. In the mouse spinal cord, the cellular response to Hh signaling is mediated primarily by the activator function of Gli2 and the repressor function of Gli3, while the activator forms of Gli1 and Gli3 also play smaller but significant roles (Bai et al., 2004; Lei et al., 2004; Motoyama et al., 2003). Glis similarly mediate Hh signaling in the zebrafish neural tube, but Gli1 is the primary activator of Hh signaling, with Gli2 and Gli3 playing minor activator and repressor roles (Karlstrom et al., 1999, 2003; Tyurina et al., 2005).

Despite this general picture of Gli function in neural patterning, the roles of the various vertebrate *Gli* genes in the formation of particular cell types such as motor neurons have not been fully resolved. In frog, misexpression of *Gli1* or *Gli2* but not *Gli3* can induce ectopic motor neurons, supporting a role for *Gli1*/*2* in motor neuron formation (Ruiz i Altaba, 1998). In the chick spinal cord, inhibition of all *Gli* activator function blocks motor neuron induction (Persson et al., 2002), and ectopic expression of Gli2 activator can induce ventral neural tube markers (Lei et al., 2004), suggesting that Gli1 and/or Gli2 activator function is necessary and sufficient for motor neuron formation. In contrast, mouse *Gli* single and double knockouts exhibit no defects in motor neuron induction. Motor neurons are induced normally in the spinal cords of *Gli1*, *Gli2*, and *Gli3* single mutants, as well as in *Gli1;Gli2*, and *Gli1;Gli3* double mutants (Ding et al., 1998; Matise et al., 1998; Park et al., 2000). Importantly, in *Gli2;Gli3* double mutants, which are essentially *Gli1;Gli2;Gli3* knockouts since *Gli1* expression is lost in these mutants, a small but significant number of spinal motor neurons differentiate although their migration and patterning are affected (Bai et al., 2004; Lei et al., 2004). In *Smo;Gli3* double mutants, which completely lack an Hh response, relatively normal numbers of motor neurons are induced at the forelimb level, while no motor neurons differentiate more posteriorly (Wijgerde et al., 2002). These results collectively indicate that while the induction of a majority of spinal motor neurons in mouse requires Gli-dependent Hh signaling, a small number of motor neurons can also be induced by Hh- and Gli-independent processes.

We therefore tested whether Gli function is absolutely necessary for motor neuron induction in zebrafish. We have been investigating the roles of Hh pathway components in motor neuron induction in zebrafish embryos using gain- and loss-of-function approaches (Bingham et al., 2001; Chandrasekhar et al., 1998, 1999). In *detour* (*dtr*) mutants (Brand et al., 1996; Karlstrom et al., 1996), induction of midbrain and hindbrain motor neurons (branchiomotor and somatomotor neurons) is completely blocked, while spinal motor neurons are induced normally

(Chandrasekhar et al., 1999). Since *dtr* encodes the zebrafish *gli1* homolog (Karlstrom et al., 2003), these results indicate that zebrafish *gli1* plays different roles in motor neuron induction in the hindbrain and spinal cord. Therefore, we were particularly interested in examining the roles of zebrafish *gli2* and *gli3* in motor neuron development. We show here that *you-too* (*yot*) mutants (Brand et al., 1996; van Eeden et al., 1996), which encode dominant repressor (DR) forms of Gli2 (Karlstrom et al., 1999; 2003), exhibit severe loss of motor neurons in the hindbrain and spinal cord. However, the motor neuron phenotype appears to be an indirect effect of mutant $Gli2^{DR}$ protein on Gli activator functions in the neural tube, since we show that wild-type *gli2* plays only a minor role in motor neuron induction within the spinal cord, and no discernable role in the hindbrain. In contrast, *gli3* plays a more prominent role in motor neuron induction in the hindbrain and spinal cord. By combining different *gli* mutants with *gli* antisense morpholinos to inhibit the function of multiple *gli* genes, we demonstrate that, unlike in mouse, Gli activator function (encoded by *gli1*, *gli2*, and *gli3*) is absolutely required for motor neuron induction at all axial levels in the zebrafish neural tube.

Materials and methods

Animals

Maintenance of zebrafish stocks and collection and development of embryos in E3 embryo medium were carried out as described previously (Chandrasekhar et al., 1997, 1999; Bingham et al., 2002; Westerfield, 1995). Throughout the text, the developmental age of the embryos corresponds to the hours elapsed since fertilization (hours post-fertilization, hpf, at 28.5° C).

You-too (yot^{ty17} and yot^{ty119}) and *slow muscle omitted* (smu^{b641}) mutants were identified on the basis of the morphology of the somites at 21 hpf (Barresi et al., 2000; van Eeden et al., 1996; Varga et al., 2001). *Detour* mutants (dtr^{te370}) were identified on the basis of defects in motor neuron development or Hh target gene expression in the hindbrain following immunohistochemistry or in situ hybridization (Chandrasekhar et al., 1999). For analysis of branchiomotor neuron development, the motor neuron-expressed *islet1-GFP* transgene (Higashijima et al., 2000) was crossed into these mutant backgrounds. Since the *islet1-GFP* reporter is not suitable for counting neuronal cell bodies, islet antibody labeling was used for quantifying motor neuron populations (see below).

Immunohistochemistry, in situ hybridization, and imaging

Whole-mount immunohistochemistry was performed with the various antibodies as described previously (Bingham et al., 2002; Chandrasekhar et al., 1997). The following antibodies were used: zn5/8 (Trevarrow et al., 1990; 1:10); islet (39.4D5; Korzh et al., 1993; 1:200); 3A10 (Hatta, 1992; 1:500). For fluorescent immunolabeling (zn5 and 3A10), RITC-conjugated secondary antibody (Jackson Immunochemicals) was used.

Synthesis of the digoxygenin- and fluorescein-labeled probes and whole-mount in situ hybridization were carried out as described previously (Bingham et al., 2003; Chandrasekhar et al., 1997; Prince et al., 1998). Two-color in situs were performed essentially as described (Prince et al., 1998) with the following modifications. After deactivating the first in situ reaction with 0.1M glycine, embryos were washed several times in 0.1M glycine before the blocking and antibody incubation steps for the second in situ probe. Fast Red substrate (Sigma) was used for the second reaction, and the substrate was replaced every 45 min until the desired color intensity was reached (usually after 5–6 hours). The following in situ probes were used: *fgf3* (Maves et al., 2002); *gli1* (Karlstrom et al., 2003); *gli2* (Karlstrom et al., 1999); *krox20* (Oxtoby and Jowett, 1993); *net1a* (Lauderdale et al., 1997); *nk2.2* (Barth and Wilson, 1995); and *ptc1* (Concordet et al., 1996).

Embryos were de-yolked, mounted in glycerol, and examined with an Olympus BX60 microscope. In all comparisons, at least ten wild-type and ten mutant embryos were examined. Confocal imaging was carried out on fixed embryos mounted in 70% glycerol. Images were captured on an Olympus IX70 microscope equipped with a BioRad Radiance 2000 confocal laser system.

Vibratome sectioning

Embryos processed for in situs were removed from 70% glycerol, rehydrated in PBS, and embedded in 7% low melting point agarose. Embryos were oriented to obtain transverse sections in the hindbrain. This process was facilitated in 15 hpf embryos (Fig. 9) by processing them for two-color in situs with *fgf3* (and *gli2*) to label the midbrain–hindbrain boundary. Since *fgf3* is also expressed in rhombomere 4 (Maves et al., 2002), the *fgf3* staining was developed very weakly to avoid interference with visualization of the *gli2* signal in the hindbrain. 50-μm-thick slices were generated using the Vibratome Plus 1000 system. The appearance of the notochord (in caudal r4) and the otic vesicle (spanning r4–r6) was monitored in successive sections and used to assign rhombomere identities to particular sections.

mRNA and antisense morpholino oligonucleotide injections

Synthesis of capped, full-length *dnPKA* mRNA (Ungar and Moon, 1996) was carried out as described previously (Chandrasekhar et al., 1998). Synthetic mRNAs were checked for purity and size by gel electrophoresis, estimated by u.v. spectrophotometry, and diluted to 400 ng/μl. mRNA (~1–2 ng/embryo) was injected into 1–8 cell stage embryos as described previously (Chandrasekhar et al., 1998, 1999).

Antisense morpholino oligonucleotides (MOs) against *gli1*, *gli2*, and *gli3* mRNA sequences were described previously (Karlstrom et al., 2003; Tyurina et al., 2005). Working dilutions of *gli1* MO (1.8 ng/nl), *gli2* MO (3 ng/nl), and *gli3* MO (10 ng/nl) were prepared in Danieu buffer, and morpholinos (5–30 ng/embryo) were injected into 1–4 cell stage embryos. The effective concentration for each morpholino was determined through dose–response experiments (see footnotes of Tables 3 and 4 for more details). Since injection of control (5 base mismatch) morpholinos had no effects on motor neuron development or Hh-regulated gene expression (see Supplementary Fig. S1), uninjected embryos served as controls in all experiments described here.

Genotyping of embryos

The tails of fixed embryos were clipped and stored in 70% glycerol. DNA was extracted for genotyping as described previously (Westerfield, 1995) with the following modifications: tail fragments were washed five times in 1 M Tris–HCl, pH 8.2 prior to digestion, and 20 μg of glycogen (Roche) was added to each sample prior to ethanol precipitation for 48 h at −20°C.

A restriction site (*Nla*III) disrupted by the yot^{ty119} point mutation (Karlstrom et al., 1999) served as an RFLP marker. PCR primers were designed (Fwd: 5′ ATG ATG CCT CAC GAA GTT CC 3′; Rev: 5′GGC AGA CGT GAT AGG TTC GT 3′) to introduce mutations to silence nearby, endogenous *Nla*III sites unaffected by the yot^{ty119} mutation. Undigested PCR products from wild-type and yot^{ty119} mutant alleles were 137 base pairs (bp) in length. *Nla*III treatment digested the PCR product from the yot^{ty119} allele into 102 bp and 35 bp fragments, and the larger fragment could be distinguished from the uncut wild-type product on a 3% agarose gel.

Cyclopamine treatment

Embryos were treated with cyclopamine (Taipale et al., 2000) as described previously (Karlstrom et al., 2003) with the following modifications. Embryos were staged and

synchronized at 5.25 hpf by discarding any embryos not at 50% epiboly. Cyclopamine stock (10 mM in 95% ethanol) was diluted to a working concentration of 100 μM in E3 medium containing 0.5% DMSO, and treated embryos were incubated in 12-well tissue culture plates.

Quantification of neuronal populations

Islet antibody-labeled nuclei of hindbrain motor neurons and neurons in the ventral spinal cord were counted in strongly labeled preparations. Counts were performed under 40× magnification. Spinal motor neurons were counted on one side in three contiguous segments at the level of the tip of the yolk tube. To determine whether observed differences were statistically significant, we performed one-way, parametric ANOVA analyses (with Bonferroni post-tests) using Graphpad Instat version 3 software (GraphPad Software, Inc.).

Results

Induction of cranial and spinal motor neurons is affected in you-too (gli2) mutants

In zebrafish *detour* (*dtr* (*gli1*$^{-}$)) mutants (Brand et al., 1996; Karlstrom et al., 1996, 2003), cranial (midbrain and hindbrain) motor neurons are not induced, while spinal motor neurons are induced normally (Chandrasekhar et al., 1999), indicating that *gli1* is necessary for cranial motor neuron induction, and suggesting that other *gli* genes may function redundantly in spinal motor neuron induction. To test this hypothesis, we examined motor neuron development and Hh-regulated gene expression in *you-too* (*yot*) mutants (Brand et al., 1996; Karlstrom et al., 1996), which encode dominant repressor forms of Gli2 (Gli2^{DR}) that block Gli1-mediated Hh signaling in reporter assays (Karlstrom et al., 1999; 2003). The characteristic organization in a wild-type embryo of the motor neurons in the midbrain (nIII, nIV) and the branchiomotor neurons in the hindbrain (nV, nVII, nX) has been described previously (Figs. 1A and D; Chandrasekhar et al., 1997; Higashijima et al., 2000). In *yot*^{ty17} mutants, midbrain motor neurons (nIII, nIV) were mostly missing, and branchiomotor neurons in the hindbrain were significantly reduced (Figs. 1B and E), consistent with the idea that Gli2^{DR} proteins block Gli1-mediated motor neuron induction. In *yot*^{ty119} mutants, branchiomotor neuron induction was even more severely affected, with the nV neurons in rhombomeres 2 and 3 (r2 and r3), and the nX neurons in the caudal hindbrain almost completely missing (Figs. 1C and F). Similarly, the zn5 antibody-labeled nVI motor neurons in r5 and r6 (Fig. 1G; Chandrasekhar et al., 1997; Trevarrow et al., 1990) were reduced in number in *yot*^{ty17} mutants (Fig. 1H), and completely lost in *yot*^{ty119} mutants (Fig. 1I). There were no observable differences in the patterns of neurogenesis (*ngn1*, *ash1a*, *ash1b*, *deltaD* expression) or cell death (acridine orange labeling) in the hindbrain between wild-type and *yot* mutant embryos (data not shown), suggesting that motor neuron induction, and not neurogenesis or cell death, is specifically affected in these mutants.

In contrast to *dtr* (*gli1*$^{-}$) mutants, *yot* (*gli2*^{DR}) mutants had reduced numbers of islet-expressing primary and secondary motor neurons in the spinal cord (Figs. 1K and L; data not shown), confirming that Gli function plays a role in spinal motor neuron induction. We quantified motor neuron loss in *yot*^{ty17} and *yot*^{ty119} mutants (36 hpf) labeled with the islet antibody and showed that these two alleles affect motor neuron induction to different degrees (Table 1). While motor neuron number was reduced ~40–50% in the hindbrain and spinal cord of *yot*^{ty17} mutants, there was a ~75% loss in *yot*^{ty119} mutants, suggesting that the *yot*^{ty119} allele encodes a more potent repressor of motor neuron induction than does the *yot*^{ty17} allele (Table 1). This is consistent with molecular identification of these alleles showing that both alleles encode truncated Gli2 proteins, with the Gli2^{ty119} protein missing more of its putative activator domain (Karlstrom et al., 1999). Interestingly, the number of motor neurons in r4–r7 (corresponding to nVI and nVII neurons in the wild-type embryo) was less reduced in *yot*^{ty119} mutants (only nVII neurons present) than were other branchiomotor neuron populations (nV, nX) (Table 1; Figs. 1A and

C). Given that nVII neurons are born in r4 and undergo tangential migration through r5 into r6 and r7 (Bingham et al., 2002), these data suggest that motor neuron induction in r4 is less severely affected than in other rhombomeres in *yot*^{ty119} mutants.

Hh signaling in r4 is largely unaffected in yot mutants

To determine the extent to which Hh signaling occurs normally in r4 of *yot* mutants, we examined the expression of several Hh target genes in the ventral hindbrain. While *nk2.2* (Barth and Wilson, 1995) was expressed without gaps along the anteroposterior (AP) axis in wild-type siblings at 21 hpf (Figs. 2A and C), its expression was almost completely eliminated in *yot*^{ty119} mutants except in r4 (Figs. 2B and D). There was a slight decrease in the number of *nk2.2*-expressing cells in r4 of mutants (Fig. 2D), but the boundaries of expression coincided precisely and reproducibly with r4 (n = 30 embryos). Similarly, the expression of *patched1* (*ptc1*; Concordet et al., 1996) was severely reduced throughout the mutant hindbrain except in r4 (Figs. 2E and F). Another Hh target, *netrin1a* (*net1a*; Lauderdale et al., 1997), is normally expressed throughout the ventral neural tube, with marked upregulation at rhombomere boundaries (Fig. 2G). In *yot*^{ty119} mutants, however, *net1a* expression was reduced in many rhombomeres (especially evident in r5 and r6) with the exception of r4 and adjacent boundaries (Fig. 2H). In cross-sections, *ptc1* was expressed ventrally in r4 in mutants, albeit in a smaller number of cells (Figs. 2I and J), while expression was completely missing in adjacent rhombomeres including r6 (Figs. 2K and L), thus highlighting the rhombomere-specific nature of this expression pattern in *yot* mutants.

We next tested whether residual *nk2.2* and *net1a* expression in r4 of *yot*^{ty119} mutants required Hh signaling using the alkaloid cyclopamine (CyA) to block Hh signaling at the level of the Smoothened receptor (Barresi et al., 2000). In ethanol-treated control embryos, the wild-type (n = 15) and mutant (n = 4) expression patterns were unaffected (Figs. 2M and N). Following CyA treatment beginning at 3 hpf, *nk2.2* expression was completely lost along the AP axis, including r4, in wild-type and mutant embryos (Fig. 2O; n = 44), demonstrating that r4-specific expression of ventral neural tube markers in *yot*^{ty119} mutants requires Hh signaling. Interestingly, blocking Hh signaling at different times had differential effects on the pattern of *net1a* expression, assayed at 30 hpf. While an early block (CyA treatment beginning at 15 hpf or earlier) blocked *net1a* expression throughout the hindbrain (Figs. 2P and Q; data not shown; n = 12), CyA treatment from 18 hpf blocked *net1a* expression in all rhombomeres except in r4 (Fig. 2R; n = 3), while CyA treatment from 24 hpf or later had no significant effect on *net1a* expression (Fig. 2S; n = 6). These observations indicate that *net1a* expression in r4 has different temporal requirements for Hh signaling and suggest that retention of Hh target gene expression in r4 of *yot* mutants may reflect the inability of the mutant Gli2 protein to block early Hh signaling in this rhombomere.

Activation of Hh signaling can alleviate defective motor neuron induction and Hh target gene expression in yot mutants

Since the *yot* alleles encode dominant repressors of Hh signaling (Karlstrom et al., 2003), we wondered whether ectopic activation of Hh signaling upstream of the Gli transcription factors by overexpression of dominant-negative protein kinase A (dnPKA; Ungar and Moon, 1996) could overcome the repressive effects of these mutations on Hh target gene (*nk2.2*, *net1a*) expression and motor neuron induction. When *dnPKA* RNA was injected into embryos from *yot*^{ty119}+/−;*islet1-GFP* crosses, there was a dramatic increase in the number of *GFP*-expressing branchiomotor neurons in all rhombomeres, and in ectopic locations along the dorsoventral axis, in ~80% of wild-type siblings (Figs. 3A and B; Table 2). Consistent with this, *nk2.2* expression was upregulated in the ventral neural tube and at ectopic locations throughout the hindbrain in ~88% of *dnPKA*-injected wild-type embryos (Figs. 3E and F). In marked contrast, no ectopic *GFP*-expressing cells were seen in *dnPKA*-injected *yot*^{ty119} mutants, but there was

a small, reproducible increase in the number of nVII neurons, and less frequently nX neurons (Figs. 3C and D; Table 2). Furthermore, while *nk2.2* was not expressed in the ventral hindbrain or in ectopic dorsal locations in *dnPKA*-injected *yot*^{ty119} mutants, its expression in ventral r4 was slightly but reproducibly upregulated (Figs. 3G and H). Interestingly, when *dnPKA* RNA was injected into embryos from *yot*^{ty17}+/−; *islet1-GFP* crosses, *net1a* was expressed ectopically in the dorsal neural tube at all axial levels in wild-type and *yot*^{ty17} mutants, but more weakly in mutants (Figs. 3I–L; Table 2). Similarly, ectopic *GFP*-expressing motor neurons and *nk2.2*-expressing cells were found in r2 and r4 of *dnPKA*-injected *yot*^{ty17} mutants (data not shown). These results suggest that while both *yot* alleles encode dominant repressors, their inhibitory activities can be overcome to different extents by hyperactivation of Hh signaling, with the *ty119* allele being more resistant to this treatment. These observations are consistent with our earlier results that the *yot* alleles represent a phenotypic series, with the *ty119* allele encoding a stronger repressor of motor neuron induction (Table 1), in accordance with reporter assays (Karlstrom et al., 2003).

Hh signaling is essential for branchiomotor neuron induction

Given that the *yot* (*gli2*^{DR}) mutations affect branchiomotor neuron number, and that Hh signaling may regulate Gli2 activator and repressor functions (Stamataki et al., 2005), we determined the overall requirement for Hh signaling in motor neuron induction, and compared it to the requirement for Gli1, which possesses only activator function (Karlstrom et al., 2003; Tyurina et al., 2005). To do this, we examined branchiomotor neuron induction and Hh-regulated gene expression in *slow muscle omitted* (*smu*^{b641}) mutants where Hh signaling is blocked due to a loss-of-function mutation in *smoothened* (*smo*) (Barresi et al., 2000; Chen et al., 2001; Varga et al., 2001), and in *detour* (*dtr*^{te370}) mutants, which carry a loss-of-function mutation in *gli1* (Karlstrom et al., 2003).

In *smu* (*smo*$^{-}$) and *dtr* (*gli1*$^{-}$) mutants, the motor neurons in the midbrain (nIII, nIV) and the branchiomotor neurons in the hindbrain (nV, nVII, nX) were almost completely missing (Figs. 4B and C; compare to Fig. 4A), demonstrating that the functions of the Smo receptor and Gli1 transcription factor are essential for their induction (see also Chandrasekhar et al., 1999). Consistent with this, the expression of several Hh-regulated genes in the hindbrain (Figs. 4D, G, J, M) was greatly reduced or completely lost in *smu* mutants (Figs. 4E, H, K, N; see also Chen et al., 2001; residual *net1a* and *gli1* expression likely due to maternally supplied Smo function). While *nk2.2* expression was similarly absent in *dtr* mutants (Fig. 4F), significant levels of *ptc1* and *net1a* expression were retained (Figs. 4I and L), indicating that some aspects of their expression do not require *gli1* function. Furthermore, *gli1* expression, which is greatly reduced in *smu* mutants, was essentially unaffected in *dtr* mutants (Fig. 4O), indicating that *gli1* expression depends on Hh signaling but does not require Gli1 function. These results demonstrate that some Hh-regulated events in the hindbrain (motor neuron induction, and expression of ventral neural tube (*nk2.2*) and motor neuron (*isl1*, *tag1*) markers (data not shown)) require *gli1* function, while others (expression of *ptc1*, *net1a*, *gli1*) do not, suggesting that other Glis (encoded by *gli2* and/or *gli3*) may activate some Hh target genes in the hindbrain (Fig. 11; Tyurina et al., 2005). Strikingly, most Hh-regulated events including motor neuron induction occur normally in the *dtr* mutant spinal cord (Chandrasekhar et al., 1999; Karlstrom et al., 2003; data not shown; see Table 3), suggesting that Glis may function in a redundant fashion in the spinal cord (Fig. 11; Tyurina et al., 2005).

Gli2 plays a minor role in spinal motor neuron induction

Given that Gli2 contributes to the Hh response in the zebrafish midbrain (Karlstrom et al., 2003), we tested whether *gli2* plays any role in motor neuron development. To knock down *gli2* function, we injected *gli2* antisense morpholinos (MOs) into embryos obtained from *yot*^{ty119}+/−;*islet1-GFP* crosses, which produce on average 25% homozygous mutant *yot*

embryos. There was no difference in the number or distribution of *GFP*-expressing motor neurons in the midbrain or hindbrain between control (16/16 embryos) and *gli2* MO-injected (57/57 embryos) wild-type siblings at 48 hpf (Figs. 5A and B; see Table 3 for quantification using islet antibody). Similarly, there were no effects on *nk2.2* expression in the ventral neural tube of 21 hpf control (43/43 embryos) and *gli2* MO-injected (25/25 embryos) wild-type siblings (Figs. 5E and F). These results demonstrate that *gli2* plays little or no role in branchiomotor neuron development.

Strikingly, loss of *GFP*-expressing motor neurons in yot^{ty119} mutants was largely rescued upon injection of *gli2* MO (Fig. 5D; 19/20 embryos; compare to control: Fig. 5C; 8/8 embryos), and motor neurons were found in all rhombomeres at their characteristic locations. This result confirms that the *gli2* MOs effectively block translation of *gli2* mRNA. Furthermore, since no full-length Gli2 protein is present in *yot* mutants, the rescue of the *yot* mutant phenotype convincingly demonstrates that branchiomotor neurons can be specified in the absence of full length, presumably activator forms of Gli2, as suggested by the normal induction of these neurons in *gli2* MO-injected wild-type embryos (Fig. 5B). Although the *yot* mutant phenotype is rescued, motor neuron numbers, especially evident for nX neurons, were still lower than in wild-type siblings. Furthermore, the nIII and nIV motor neurons in the midbrain never reappeared in *gli2* MO-injected mutants. Consistent with these results, *nk2.2* expression was restored in large regions of the ventral hindbrain, but never in the midbrain, of *gli2* MO-injected *yot* mutants (Fig. 5H; 8/8 embryos; control, Fig. 5G: 11/11 embryos). Therefore, the incomplete rescue of the mutant phenotype in the midbrain and hindbrain of *gli2* MO-injected *yot* mutants may reflect substantial, but not complete, knockdown of $Gli2^{DR}$ synthesis.

If Hh-regulated events could be mediated redundantly by activator functions of Gli1, Gli2, and Gli3 (see model in Fig. 11), the lack of a phenotype in *gli2* MO-injected wild-type embryos may merely reflect the relative contributions of the various Glis in mediating specific events. In this case, we would predict that minor roles for the Gli2 activator would be discernable in the absence of functional Gli1. We therefore examined Hh-regulated events in the hindbrain and spinal cord of *detour* ($gli1^{-}$) mutants following *gli2* MO injection. The number of islet antibody-labeled motor neurons in the spinal cord was reproducibly and significantly reduced by ~25% in *gli2* MO-injected *dtr* mutants (Fig. 5L; Table 3) compared to those in uninjected and *gli2* MO-injected wild-type embryos, and uninjected *dtr* mutants (Fig. 5K; Table 3). Furthermore, the residual, but substantial, expression of *net1a* in the *dtr* mutant hindbrain (Figs. 1L and 5I; $n = 15$ embryos) was either slightly reduced or unaffected following *gli2* MO injection (Fig. 5J; 21/21 embryos), and *net1a* expression was unaffected in wild-type siblings injected with *gli2* MO ($n = 40$) as seen for *nk2.2* (Figs. 5E and F). These observations suggest strongly that although *gli2* appears to play no role in motor neuron induction or Hh target gene activation in the hindbrain, Gli2 activator function is needed for inducing some spinal motor neurons.

Dominant repressor Gli2 blocks motor neuron induction by interfering with Gli1 function

If motor neuron loss in *yot* mutants were a consequence of $Gli2^{DR}$-mediated interference with Gli1 activator function in hindbrain, and with Gli1 and other Gli activator functions in the spinal cord (see Fig. 11), one would predict that the *yot* ($gli2^{DR}$) mutant motor neuron phenotype would be exacerbated upon reduction of Gli1 activator function. We tested this by injecting *gli1* MO into embryos obtained from yot^{ty119}+/– crosses, and examining motor neuron development with islet antibody labeling (Fig. 6; Table 4). In wild-type (*gli2*+/+) embryos, injection of a sub-optimal amount of *gli1* MO (Karlstrom et al., 2003) did not result in a discernable loss of motor neurons in the hindbrain or spinal cord, and the embryos looked identical to control *gli2*+/+ embryos (Figs. 6A and I; data not shown; Table 4). In contrast, *gli1* MO injection into *gli2* heterozygotes (*gli2*+/DR) led to a substantial loss of hindbrain

motor neurons (Fig. 6B), with the pattern of loss greatly resembling that found in control *yot* (*gli2* DR/DR) mutants (Fig. 6C). However, unlike in the hindbrain, spinal motor neuron loss was less severe in *gli1* MO-injected *gli2* heterozygotes (Fig. 6J) compared to *yot* mutants (Fig. 6K; Table 4). Finally, as predicted, *gli1* MO injection into *yot* mutants led to the complete loss of motor neurons in the hindbrain and spinal cord (Figs. 6D and L; Table 4), similar to the phenotype of *smu* mutants and cyclopamine-treated embryos (data not shown). These results suggest strongly that the $Gli2^{DR}$ protein affects motor neuron development by interfering with the activator functions of Gli1, Gli2, and possibly other Glis (Fig. 11).

Our earlier observations that significant levels of *net1a* and *ptc1* expression are retained in *yot* and *dtr* mutants (Figs. 2 and 4; Fig. 6G) and in *gli2* MO-injected *dtr* mutants (Fig. 5J) suggested that Gli activator-independent mechanisms may be involved in regulating their expression. However, step-wise reduction of Gli activator function by *gli1* MO injection into *gli2* heterozygotes (*gli2*+/DR; 15/25 embryos) and *yot* mutants (*gli2* DR/DR; 9/13 embryos) led to additive losses in *net1a* expression (Figs. 6F and H), suggesting strongly that Gli activator function is necessary for regulating all aspects of *net1a* (Fig. 6) and *ptc1* (see Fig. 10) expression.

Gli3 plays a role in branchiomotor and spinal motor neuron induction

Given the redundant functions of *gli1* and *gli2* in spinal motor neuron induction, we tested whether zebrafish *gli3* (Tyurina et al., 2005) also contributed to motor neuron induction. Since the roles of *gli1* and *gli2* in spinal motor neuron induction were revealed only in Gli-deficient backgrounds (Figs. 5 and 6), we examined the effects of knocking down *gli3* function using *dtr* (*gli1*$^{-}$) and *yot* (*gli2*^{DR}) mutants. We first verified that *gli3* MO injection indeed knocked down *gli3* function by showing that ~36% of wild-type embryos injected with 30 ng *gli3* MO exhibited ectopic expression of the floor plate marker *fkd4* in the dorsal hindbrain, as described previously (Tyurina et al., 2005; data not shown; 24/66 embryos). Interestingly, injection of *gli3* MO into wild-type siblings of *dtr* or *yot* mutants led to significant reductions in both branchiomotor (Figs. 7B and J; compare to Figs. 7A and I) and spinal motor neurons (Figs. 7F and N; compare to Figs. 7E and M) (Tables 3 and 4), suggesting that *gli3* plays a more prominent role than *gli2* in motor neuron induction. In *dtr* (*gli1*$^{-}$) mutants injected with *gli3* MO, while the severe loss of branchiomotor neurons seen in control embryos was maintained (Figs. 7C and D; Table 3), spinal motor neurons were greatly reduced compared to control mutant embryos (Figs. 7G and H; Table 3). This result suggests an activator role for Gli3 in spinal motor neuron induction. In *yot* (*gli2*^{DR}) mutants injected with *gli3* MO, there was a small decrease in branchiomotor neuron number compared to control embryos (Figs. 7K and L; Table 4), but a dramatic reduction in spinal motor neuron number over control mutant embryos (Figs. 7O and P; Table 4). This result again suggests an activator function for Gli3 in spinal motor neuron induction, and that this function may be subject to interference from $Gli2^{DR}$ protein. In addition, Gli3 may regulate motor neuron induction indirectly by activating *gli1* expression (see Figs. 10 and 11, and Discussion). These results also suggest that Gli3 does not function as a repressor of motor neuron fate in the dorsal neural tube. But we cannot rule out other roles for *gli3* in hindbrain development because the fourth ventricle (above the hind-brain) was variably reduced in *gli3* MO-injected embryos, and the hindbrain had a mottled appearance suggestive of increased cell death (data not shown). Expression of *ptc1* and *krox20* (Fig. 10K) however was unaffected in these embryos.

Endogenous Gli2 repressor function does not regulate branchiomotor neuron induction

While wild-type *gli2* appears to play no role in branchiomotor neuron induction (Fig. 5; Table 3), the Gli2 dominant repressors encoded by the *yot* alleles interfere with branchiomotor neuron induction (Figs. 1 and 6; Tables 1 and 4). Therefore, we wondered whether endogenous Gli2 repressor activity normally plays any role in branchiomotor neuron development, analogous

to the role of Gli3 repressor function in ventral neural tube patterning in mouse (Litingtung and Chiang, 2000;Wijgerde et al., 2002). In a 21 hpf wild-type hindbrain, the *islet1* expression domain (presumptive motor neurons) in rhombomere 4 (r4) and the *nk2.2* expression domain (containing presumptive motor neurons) in r5 were located in the ventral-most neural tube, outside the *gli2* expression domain (Figs. 8A and E). This dorsal pattern of *gli2* expression is evident from 16.5 hpf until 36 hpf (data not shown; Karlstrom et al., 1999), the time period when most of the branchiomotor neurons differentiate (Chandrasekhar et al., 1997;Higashijima et al., 2000). This absence of expression in differentiating motor neurons suggests that *gli2* does not directly influence motor neuron induction at these time points. However, since motor neurons are clearly affected in *smu*, *dtr*, and *yot* mutants, this suggests either that (1) *gli2* (and therefore Gli2 or $Gli2^{DR}$ proteins) is aberrantly expressed in the ventral hindbrain (in motor neuron progenitors) in these mutants, (2) *gli2* indirectly affects motor neuron induction, or (3) Gli-mediated motor neuron differentiation occurs prior to 16.5 hpf at a time when *gli2* is expressed in motor neuron progenitors.

To distinguish between these possibilities, we first tested whether branchiomotor neuron loss in *smu*, *dtr*, and *yot* mutants might result from the ventral expansion of *gli2* expression into regions containing motor neuron progenitors. We examined the expression domains of *gli2* at various levels along the AP axis in 21 hpf mutant embryos processed for *gli2;islet1* double in situ hybridization. There was no significant or reproducible ventral expansion of *gli2* expression in the neural tube at hindbrain levels in any rhombomere in any of the three mutant backgrounds (4–6 embryos examined per mutant, 5–6 sections in the hind-brain per embryo). In the various mutants containing few (Fig. 8B) or no *islet1*-expressing cells (Figs. 8C and D), or no *nk2.2*-expressing cells (Fig. 8F), *gli2* expression was clearly excluded from the ventral neural tube containing the motor neuron progenitor domain. There was no ventral expansion of *gli2* expression in the hindbrains of *smu* (21 and 26 hpf), *dtr* (18 and 21 hpf), and *yot* mutants (16.5, 18, 21, and 26 hpf) (data not shown). Together, these data suggest strongly that the loss of branchiomotor neurons in these Hh pathway mutants is not due to the suppression of motor neuron fate by Gli2 repressor function but may simply be due to loss of Gli1 activator function (Figs. 4M–O; see Fig. 11 for model). Interestingly, *gli2* expression expands ventrally in the forebrain of Hh pathway mutants. In cross sections of the forebrain at the level of the epiphysis, *gli2* was expressed in the dorsal ~65% of the neural tube in wild-type embryos (Fig. 8G; Table 5). In all mutants examined, the *gli2* expression domain at the forebrain level was expanded ventrally (and reproducibly) to 75–90% of the extent of the neural tube (Figs. 8H–J; Table 5), demonstrating a significant effect on dorsoventral patterning when Hh signaling is reduced or absent. Therefore, the reduction or loss of Hh target gene expression in the forebrain in Hh pathway mutants may result from Gli2-mediated repression.

To test the possibility that Gli2 repressor function in the dorsal neural tube has an indirect effect on Hh-mediated events in the ventral neural tube, we asked whether knockdown of *gli2* function could rescue any aspect of Hh signaling, including branchiomotor neuron induction, in *smu* mutants, in a manner similar to the rescue of motor neurons in *Shh;Gli3* and *Smo;Gli3* mutant mice (Litingtung and Chiang, 2000; Wijgerde et al., 2002). When *gli2* MO was injected into embryos from a *smu+/−;islet1-GFP* incross, branchiomotor neurons did not reappear in *smu* mutants, and there was no rescue of *nk2.2* or *net1a* expression in the mutant hindbrain (data not shown), consistent with the idea that Gli2 repressor function in the dorsal hindbrain does not influence Hh-mediated events in the ventral hindbrain.

Finally, we tested the possibility that the loss of motor neurons in *yot* mutants could result from the ventral expression of *gli2* (and $Gli2^{DR}$) in motor neuron progenitors before 16.5 hpf. *Gli2* was expressed extensively in the neural plate and the developing neural tube at 9 and 12 hpf (data not shown), and continued to be expressed in the ventral neural tube at 15 hpf throughout the hindbrain (Figs. 9A–C). These results indicate that aberrant $Gli2^{DR}$ activity in

motor neuron progenitors before 15 hpf can account for reduced motor neuron induction in *yot* mutants and suggest that branchiomotor neurons are specified before 15 hpf, which is several hours earlier than suggested by observations of motor neuron differentiation (Chandrasekhar et al., 1997; Higashijima et al., 2000).

Hh signaling is primarily required before 18 hpf to induce branchiomotor neurons

Given that $Gli2^{DR}$ proteins block motor neuron induction in *yot* mutants by interfering with Gli1 and Gli3 function, and that *gli1* and *gli2* are co-expressed in motor neuron progenitors only before 16.5 hpf, we re-examined the idea that the branchiomotor neurons are specified continuously between 15 and 40 hpf (Chandrasekhar, 2004). To determine directly the critical period for motor neuron induction, we asked when different subsets of branchiomotor neurons were specified using the alkaloid cyclopamine (CyA) to block Hh signaling. Wild-type *islet1-GFP* transgenic embryos were treated with CyA beginning at 3, 6, 9, 12, 15, 18, 21, and 24 hpf. Control (EtOH-treated) and CyA-treated embryos were scored for motor neuron phenotypes at 48 hpf by examining *GFP* expression (Figs. 9D and E), fixed and processed for islet immunohistochemistry (Figs. 9F–I), and motor neurons in various rhombomeres (corresponding to specific types of branchiomotor neurons) were counted. CyA treatment at 9 hpf or earlier led to the complete loss of all branchiomotor neurons (Figs. 9D–G). However, a few nV neurons (in r2 and r3), and nVII neurons (in r4–r7) were generated between 9 and 12 hpf (Fig. 9H). Indeed, normal numbers of nV neurons were generated in r2 even when Hh signaling was blocked from 18 hpf (Figs. 9D and I). Similarly, a majority of nVII neurons were generated in 18 hpf-treated embryos (Figs. 9E and I), and essentially normal numbers of nV neurons (r2 and r3) and nVII neurons (r4–r7) are generated in 24 hpf-treated embryos (data not shown). These results demonstrate that Hh signaling is required before 24 hpf for generating all branchiomotor neurons, and that a majority of branchiomotor neurons are specified before 18 hpf, consistent with an early inhibitory role for mutant $Gli2^{DR}$ proteins within motor neuron progenitors in *yot* mutants.

Gli3, but not Gli1 or Gli2, activator function is required for inducing gli1 expression

We showed earlier that while *gli1* expression is completely normal in *detour* (*gli1*$^{-}$) mutants, it is severely reduced in *smu* (*smo*$^{-}$) mutants, demonstrating that *gli1* expression is regulated by Hh signaling but does not require Gli1 activator function (Fig. 4). Similarly, while *Gli1* expression is unaffected in *Gli1* knockout mouse embryos (Park et al., 2000), it is completely lost in *Gli2;Gli3* double knockout embryos (Bai et al., 2004). To test the potential role of Gli activator function in regulating *gli1* expression in zebrafish, we examined *ptc1* and *gli1* expression in conditions where overall Gli activator function was greatly attenuated (Fig. 10). In the first set of experiments, embryos from *dtr*^{te370}+/– crosses were injected with *gli2* MO that leads to a reduction of motor neurons in the spinal cord (see Fig. 5). In uninjected (21/21 embryos) and *gli2* MO-injected (36/36 embryos) wild-type siblings, *ptc1* expression in the ventral hindbrain was unaffected (Fig. 10A), indicating that the reduction in Gli activator function was not sufficient to reduce *ptc1* expression. In contrast, *ptc1* expression was reduced in uninjected *dtr* mutants (Fig. 10B; 5/5 embryos; see also Fig. 4I), and severely reduced in *gli2* MO-injected *dtr* mutants (Fig. 10C; 14/14 embryos), indicating that the Gli activator functions encoded by *gli1* and *gli2* are necessary for inducing *ptc1* expression. As expected, there was no effect on *gli1* expression in *gli2* MO-injected wild-type embryos (Fig. 10D). Surprisingly, *gli1* expression was completely normal in *gli2* MO-injected *dtr* mutants (Fig. 10E), indicating that a severe reduction in Gli1 and Gli2 activator function could not alter *gli1* expression. In a second set of experiments, embryos from *yot*^{ty119}+/– crosses were injected with *gli1* MO that leads to a severe loss of motor neurons in the hindbrain and spinal cord (see Fig. 6). While *ptc1* expression was normal in control (17/17 embryos) and *gli1* MO-injected wild-type (Fig. 10F; 20/20 embryos), the lower level of *ptc1* expression seen in uninjected *yot* mutants (Fig. 10G; 5/5 embryos) was almost eliminated in *gli1* MO-injected *yot* mutants

(Fig. 10H; 3/3 embryos). Most importantly, *gli1* expression was not affected in *gli1* MO-injected *yot* mutants (compare Figs. 10I and J). These results again indicate that conditions that lead to severe attenuation of overall Gli activator function, such that the expression of Hh target genes *net1a* (Fig. 6) and *ptc1* is severely reduced, are still unable to alter *gli1* expression.

Since we have defined an activator function for Gli3 in motor neuron induction (Fig. 7), we next tested whether Gli3 may regulate *gli1* expression by injecting *gli3* MO into embryos from dtr^{te370}+/− crosses and yot^{ty119}+/− crosses. *Gli1* was expressed normally in all wild-type and *dtr* mutant embryos injected with *gli3* MO, and the expression patterns were indistinguishable from those in control embryos (69/69 control and 49/49 *gli3* MO-treated embryos; data not shown; see Figs. 10D and E for expression patterns). These data indicate that a dose of *gli3* MO that knocks down *gli3* expression (function) substantially enough to reduce motor neuron induction (Fig. 7) is not able to affect *gli1* expression. Similarly, *gli1* expression appeared normal in *gli3* MO-injected wild-type siblings obtained from yot^{ty119}+/− crosses (Figs. 10N and O; 124/124 embryos). Significantly, *gli1* expression was greatly reduced throughout the ventral neural tube in *yot* mutants injected with *gli3* MO (Fig. 10P; 37/37 embryos). Since loss of Gli1 and Gli2 activator function alone and in combination had no effect on *gli1* expression, these data suggest that the combined effect on Gli3 function produced by $Gli2^{DR}$-mediated interference and *gli3* MO knockdown is responsible for the observed reduction in *gli1* expression. While *ptc1* expression was slightly reduced in some *gli3* MO-injected wild-type siblings (Fig. 10K; 13/36 embryos) compared to control wild-type siblings (data not shown; 28/28 embryos; see Fig. 10F), its expression was almost eliminated in *gli3* MO-injected *yot* mutants (Fig. 10M; 13/15 embryos) compared to control mutant embryos (Fig. 10L; 9/9 embryos). Collectively, these results suggest strongly that Gli activator functions encoded by *gli1*, *gli2*, and *gli3* are all equally capable of inducing *ptc1* expression, whereas Gli3 activator function is specifically required for inducing *gli1* expression (Fig. 11).

Discussion

Role of Glis in motor neuron development

In mouse and zebrafish, loss of Smoothened-mediated Hh signaling results in the failure of motor neuron induction (Chen et al., 2001; Varga et al., 2001; Wijgerde et al., 2002; this study). Nevertheless, a small number of motor neurons differentiate but are patterned abnormally in mice lacking all Gli activator function (Bai et al., 2004; Lei et al., 2004). Moreover, while mouse *Gli1* function is not required for motor neuron induction (Park et al., 2000), zebrafish *gli1* is essential for motor neuron induction in the hindbrain (Chandrasekhar et al., 1999). Given these differing roles for *gli1* in Hh-mediated motor neuron induction in zebrafish and mouse, we tested in this study whether other zebrafish *glis* such as *gli2* and *gli3* played any role in this process, and particularly whether Gli activator function was essential for motor neuron induction in zebrafish. We have addressed these questions by examining the motor neuron phenotypes of *you-too* (*yot*) mutants, which carry mutations in *gli2* (Karlstrom et al., 1999, 2003), and of embryos treated with antisense morpholinos to knockdown specific *gli* function. Our results demonstrate that, unlike mouse, Gli activator function is absolutely required for motor neuron induction at all axial levels in zebrafish.

The you-too (yot) motor neuron phenotype

The *yot* mutants were originally identified on the basis of defects in somite patterning, midline defects in the spinal cord, and defective retinotectal projections (Brand et al., 1996; Karlstrom et al., 1996; van Eeden et al., 1996). The *yot* locus encodes Gli2, which contains both C-terminal activator and N-terminal repressor domains (Karlstrom et al., 1999). The yot^{ty119} and yot^{ty17} alleles encode C-terminally truncated proteins that appear to function as dominant repressors (DR) of Hh signaling (Karlstrom et al., 1999, 2003). In contrast, Gli1, encoded by the *detour*

(*dtr*) locus, appears to lack the N-terminal repressor domain, and functions only as a transcriptional activator (Karlstrom et al., 2003). Consistent with this, extant *gli1* mutant alleles encode C-terminally truncated proteins missing the activator domains and exhibit no biological activity in reporter assays (Karlstrom et al., 2003).

In both *yot* alleles, there is a reduction in motor neuron number in the hindbrain and spinal cord, with the yot^{ty119} allele exhibiting a more severe phenotype (Fig. 1; Table 1), consistent with the stronger dominant suppressor function of this allele in the transcriptional reporter assay (Karlstrom et al., 2003). The yot^{ty119} mutants also exhibit more severe defects than yot^{ty17} mutants in the expression of Hh-regulated genes (Fig. 2; data not shown). Nevertheless, motor neuron number and Hh-regulated gene expression are not noticeably reduced in embryos heterozygous for either allele, except for a slight but consistent defect in *nk2.2* expression in the yot^{ty119}+/− hindbrain (data not shown). These results suggest that the mutant $Gli2^{DR}$ proteins cannot significantly affect Gli1 and Gli2 activator function when multiple copies of the wild-type genes (*gli1* and *gli2*) are present. Consistent with this idea, hyperactivation of Hh signaling by misexpression of dominant-negative protein kinase A (dnPKA) leads to a substantial recovery of motor neuron number and Hh target gene expression in the hindbrain of yot^{ty17}, and to a lesser extent yot^{ty119}, mutants (Fig. 3; Table 2), presumably by upregulating the level of Gli1 activator.

Strikingly, expression of many Hh target genes is greatly reduced throughout the yot^{ty119} mutant hindbrain, except in rhombomere 4 (Fig. 2). Residual gene expression in r4 is still Hh-dependent since cyclopamine treatment completely blocks expression in mutant embryos. The cyclopamine inhibitor experiments also reveal that r4-specific expression of Hh target genes (the yot^{ty119} phenotype) can be phenocopied by cyclopamine treatment beginning at 18 hpf, suggesting that the yot^{ty119} mutant phenotype may reflect the failure of Hh signaling at different times in different rhombomeres. Furthermore, ectopic Hh pathway activation through *dnPKA* overexpression in yot^{ty119} mutants leads to a consistent upregulation of *nk2.2* expression within the normal ventral domain, but not at ectopic locations in r4 (Fig. 3). These observations collectively suggest that the Hh signaling environment in r4 is different from that in adjacent rhombomeres, which is not surprising given that r4 develops earlier than adjacent rhombomeres, and functions as an organizer to signal to and regulate the patterning of these compartments (Maves et al., 2002).

Gli1, Gli2, and Gli3 activators contribute to the induction of spinal motor neurons

The normal induction of spinal motor neurons in *dtr* ($gli1^{-}$) mutants (Chandrasekhar et al., 1999) suggests that Gli activator function provided by Gli1, Gli2, and Gli3 can function in a redundant fashion in the spinal cord. We tested this idea by knocking down *gli1* or *gli3* function in *yot* mutants, which led to the complete loss of motor neurons in the spinal cord (Figs. 6 and 7), indicating that Gli1 and Gli3 activators can contribute to spinal motor neuron induction (Fig. 11).

Since knockdown of *gli2* function in wild-type embryos did not reveal any defects in motor neuron development, we sought potential roles for *gli2* in sensitized conditions where the total level of Gli activator was reduced. Therefore, we examined the consequences of *gli2* knockdown in *dtr* ($gli1^{-}$) mutants. While normal numbers of spinal motor neurons develop in *dtr* mutants (Chandrasekhar et al., 1999; Fig. 5; Table 3), there is a small (~25%) but significant reduction in motor neuron number following *gli2* MO injection, demonstrating that Gli2 contributes to spinal motor neuron induction. Since hindbrain motor neurons are essentially absent in *dtr* mutants (Chandrasekhar et al., 1999), it is unlikely that *gli2* plays any role in their formation. In contrast to *gli2*, knockdown of *gli3* led to loss of both branchiomotor (hindbrain) and spinal motor neurons in wild-type embryos, and in the *dtr* ($gli1^{-}$) and *yot* ($gli2^{DR}$) mutant spinal cords (Fig. 7), indicating that Gli3 activator function plays a more prominent role than

Gli2 in motor neuron induction. Moreover, *gli2* knockdown in *dtr* mutants or *gli3* knockdown in *dtr* or *yot* mutants led to the loss of residual *ptc1* expression in the hindbrain (Fig. 10), consistent with the minor activator roles for both Gli2 and Gli3 in Hh signaling shown previously (Karlstrom et al., 2003; Tyurina et al., 2005). Thus the residual expression of *net1a* (Fig. 5) and *ptc1* seen in *dtr* (*gli1*$^{-}$) mutants appears to result from the activator functions of Gli2 and Gli3 (Fig. 11). Importantly, our data now show that Gli3 activator function is also critical for the induction of a distinct ventral cell type, namely motor neurons.

Knockdown of *gli2* function alone had no effect on the induction of hindbrain and spinal motor neurons (Fig. 5; Table 3). Since motor neuron number is a measure of floor plate- and notochord-derived Hh activities (Chandrasekhar et al., 1998), this suggests that the development of the floor plate and other ventral cell types does not require Gli2 activity. Consistently, *nk2.2*-expressing medial and lateral floor plate cells are unaffected in *gli2* MO-injected wild-type embryos (Karlstrom et al., 2003). In contrast, mouse *gli2* is essential for development of the floor plate and adjacent cells (Ding et al., 1998;Matise et al., 1998), reflective of the functional divergence in Gli2 reported earlier (Karlstrom et al., 2003). Although spinal motor neurons develop normally in mouse *Gli2* mutants due to notochord-derived Hh signals (Ding et al., 1998;Matise et al., 1998), it is not known whether mouse *Gli2* is required for motor axon outgrowth, in a similar fashion to zebrafish *gli2* (Brand et al., 1996;Zeller et al., 2002).

In this report, we have tested whether *gli2* and *gli3* are required for motor neuron induction. Our data suggest important roles for the activator forms of both Gli2 and Gli3 in this process. In mouse, a *Gli1* knock-in (encoding only Gli activator function) can rescue *Gli2* mutant phenotypes, indicating that loss of Gli2 activator function is responsible for the phenotypes seen in *Gli2* mutants (Bai and Joyner, 2001; Bai et al., 2002). Consistent with this, knockdown of zebrafish *gli2* function in *smu* (*smo*$^{-}$) mutants does not abrogate defective Hh-regulated events, including motor neuron induction, suggesting that the repressor function of zebrafish Gli2 does not play a significant role in Hh-regulated patterning in the hindbrain. Nevertheless, we cannot rule out that some of the effects on zebrafish spinal motor neuron development following *gli2* knockdown are indirect effects of the repressor function of Gli2. Similarly, while our data suggest strongly that Gli3 activator function contributes to branchiomotor and spinal motor neuron induction (Fig. 7), it is formally possible that Gli3 repressor function may influence motor neuron fate in the hindbrain. These ideas will be tested in the future through *gli* gain-of-function and *gli2;gli3* double knockdown experiments.

Differential requirements for Gli activator function in mouse and zebrafish

While Gli2 repressor function appears to be dispensable for neural tube patterning in both mouse and zebrafish, it appears that Gli activator functions have profoundly different roles during motor neuron development in the two species. We have shown here that zebrafish *gli1*, *gli2*, and *gli3* can contribute to spinal motor neuron induction. Furthermore, we showed previously that zebrafish *gli1* is essential for the development of all motor neurons in the midbrain and hindbrain (Chandrasekhar et al., 1999; A.C., unpublished data), and we show here that *gli3* also plays a role in hindbrain motor neuron induction. In sharp contrast, analysis of specific *Gli* single and double knockouts suggested that Gli activator function is not required for the induction of motor neurons in the mouse spinal cord (Ding et al., 1998; Matise et al., 1998; Park et al., 2000). In mouse *Gli2;Gli3* double knockouts (which are essentially *Gli1;Gli2;Gli3* triple knockouts, since *Gli1* is not expressed in the double mutant), motor neuron progenitors are found in normal numbers, while the number of differentiated motor neurons is much smaller, and they exhibit patterning and migration defects (Bai et al., 2004; Lei et al., 2004). These and other results from *Shh;Gli3* (Litingtung and Chiang, 2000) and *Smo;Gli3* (Wijgerde et al., 2002) knockout mice suggest that spinal motor neurons can be

induced in small numbers by stochastic, Gli/Hh-independent mechanisms, likely through retinoid signaling (Novitch et al., 2003). It should also be noted that since motor neuron development at more rostral levels (in the brainstem) was not examined in any of these compound mutants, Gli activators may yet be found to play a role in motor neuron induction in the mouse head, similar to zebrafish.

Why do *Gli* knockout mice and *gli* knockdown or mutant zebrafish exhibit significantly different motor neuron phenotypes? Specifically, mouse *Gli1* knockout mice develop motor neurons normally (at all axial levels) and are viable (Park et al., 2000), while zebrafish *detour* (*gli1*$^{-}$) mutants specifically fail to generate cranial motor neurons (Chandrasekhar et al., 1999) and die as embryos (Karlstrom et al., 1996). In *Gli1* mutant mice, *Gli2* and *Gli3* are expressed ventrally, and their activator functions compensate for the loss of Gli1 activity (Bai et al., 2004; Lei et al., 2004). In contrast, while *gli2* and *gli3* are transiently expressed in the ventral neural tube within the normal *gli1* expression domain in *dtr* (*gli1*$^{-}$) mutants (this study; Karlstrom et al., 1999, 2003; Tyurina et al., 2005), the absence of hindbrain motor neurons in this mutant suggests that Gli2 and Gli3 activator functions cannot compensate for the loss of Gli1 activator function. This hypothesis can be tested through gain-of-function experiments (see below). Interestingly, *gli3* knockdown results in decreased numbers of hindbrain motor neurons, suggesting a role for Gli3 activator in their induction (Fig. 7). However, given the *dtr* motor neuron phenotype, the role for zebrafish *gli3* in branchiomotor neuron induction is likely to be indirect, since *gli3* function is needed for inducing *gli1* expression (Fig. 10).

Unlike the dramatic difference in cranial motor neuron phenotypes between mouse and fish *Gli1* mutants, there is a significant but subtler difference in spinal motor neuron phenotypes between the mouse *Gli* "triple" knockout and the zebrafish *gli2*$^{DR/DR}$;*gli1* MO and *gli2*$^{DR/DR}$;*gli3* MO embryos. Differentiated, Islet^{+} motor neurons in the spinal cord are greatly reduced in number, but not completely missing in the *Gli2;Gli3* mutant mice (Lei et al., 2004), whereas they are essentially lost in the zebrafish *gli2*$^{DR/DR}$;*gli1* MO and *gli2*$^{DR/DR}$;*gli3* MO embryos (Figs. 6 and 7). While the number of Olig2^{+} spinal motor neuron progenitors in the mutant mice is unaffected, mouse Gli activator function seems to be especially important for the differentiation of these progenitors and patterning of motor neurons (Bai et al., 2004; Lei et al., 2004). Since retinoic acid (RA) signaling can independently generate progenitor domains in the mouse ventral spinal cord (Novitch et al., 2003), it is possible that the small number of motor neurons differentiating in the mutant mice also result from RA-dependent mechanisms. We have not tested whether *olig2*-expressing spinal motor neuron progenitors (Park et al., 2002, 2004) form normally in zebrafish *gli2*$^{DR/DR}$;*gli1* MO and *gli2*$^{DR/DR}$;*gli3* MO embryos, as in the mutant mice. However, it is clear that even if the progenitors are formed, they are unable to differentiate into motor neurons in the absence of Gli1, Gli2, and Gli3 activator function.

While our studies address whether zebrafish *gli1*, *gli2*, and *gli3* are necessary for motor neuron induction, they provide no insight into whether zebrafish *glis* have different abilities to induce motor neurons, or whether *gli1*-, *gli2*-, and *gli3*-encoded activator functions are equivalent. Activator forms of mouse Gli2 and Gli3 have distinct abilities to induce ventral cell fates when expressed ectopically in the chick neural tube, with Gli2 generating a broader range of cell types (Lei et al., 2004). In addition, mouse *Gli3* expressed from the *Gli2* promoter cannot fully rescue the *Gli2* knockout phenotype (Bai et al., 2004). In contrast, mouse *Gli1* expressed from the *Gli2* promoter can fully rescue the *Gli2* knockout phenotype (Bai and Joyner, 2001). These results indicate that mouse Glis have varying degrees of overlapping activator functions. It will be of interest to test whether zebrafish Glis similarly share some functionality. Furthermore, given that zebrafish Gli1 is essential for motor neuron induction while mouse Gli1 is not, it would be instructive to test whether mouse Gli1 can participate in motor neuron formation in zebrafish. These experiments will reveal whether the different abilities of the Gli1 orthologs

to induce motor neurons reflect differences in activity levels as proposed (Stamataki et al., 2005), or more fundamental differences in their abilities to induce the motor neuron fate.

Early role for Hh signaling in branchiomotor neuron induction

In seeking to explain the loss of branchiomotor neurons in *yot* mutants, we discovered that these neurons are specified very early during embryogenesis. In zebrafish, the reticulospinal interneurons and a few, large spinal motor neurons are specified by the end of gastrulation and represent the earliest-born (primary) neurons (Mendelson, 1986; Eisen, 1991). By contrast, smaller and more numerous spinal motor neurons are specified in a secondary wave of neurogenesis during somitogenesis and later stages (Kimmel and Westerfield, 1990). The branchiomotor neurons have been generally regarded as later-born secondary neurons since the earliest differentiated neurons appear around 15 hpf, and their numbers increase continuously until 36–40 hpf (Chandrasekhar et al., 1997; Higashijima et al., 2000; Linville et al., 2004). Therefore, we were surprised when the cyclopamine experiments (Fig. 8) revealed that Hh signaling specifies virtually all branchiomotor neurons prior to 15 hpf. A significant number of nV and nVII neurons are specified between 6 and 12 hpf, spanning gastrulation. Blocking Hh signaling after 18 hpf has no effect on the induction of any branchiomotor neuron subtype including the nX neurons, most of which appear between 30 and 40 hpf. Interestingly, BrdU labeling reveals that many nV and nVII neuronal progenitors remain in S-phase at 18 and 21 hpf (A.C., unpublished), several hours after Hh signaling has specified their formation. The temporal lag between the critical period of Hh sensitivity and the appearance of differentiated neurons likely reflects the time needed for motor neuron progenitors to undergo an orderly process of specification, cell-cycle exit, and differentiation involving the expression of numerous regional (e.g., *pax6*) and cell-type specific (e.g., *nk2.2*, *olig2*) transcription factors, in a manner similar to that described for spinal motor neurons in chick and mouse (reviewed in Shirasaki and Pfaff, 2002). In addition to Hh-mediated signaling, retinoic acid (RA) also appears to play a role in inducing branchiomotor neurons, especially the nX motor neurons (Begemann et al., 2004; Linville et al., 2004), mirroring the parallel roles of Hh and RA signaling in the formation of motor neuron progenitor domains in the mouse spinal cord (Novitch et al., 2003). However, our results suggest that RA signaling cannot induce any branchiomotor neurons in the absence of Gli-mediated Hh signaling. It will be of interest to determine the relationship between these signaling pathways during motor neuron induction in zebrafish.

In summary, while a small number of motor neurons can be induced by Hh- and Gli-independent processes in mouse, our data demonstrate an absolute requirement for Gli activator function in the formation of motor neurons at all axial levels in zebrafish. Furthermore, our data have identified separable roles for Gli1, Gli2, and Gli3 activator functions in motor neuron induction. Thus while the overall requirement for Gli function in motor neuron induction is largely conserved between zebrafish and mouse, the roles of particular Gli family members in this process appear to have diverged. Whether this functional divergence reflects changes in gene expression patterns, changes in level of protein activity, and/or changes in protein function remains to be determined.

Acknowledgements

We thank Michael Matise for critically reading the manuscript. We thank Andy McClellan for help with statistical analysis, and Steve Devoto for the *smu*^{b641} carrier fish. We thank Amy Foerstel, Moe Baccam, Keqing Zhang, Matthew McClure, and Vinoth Sittaramane for excellent fish care, and Stephanie Bingham and Rhituparna Chatterjee for capturing some images. We thank Jim Lauderdale, Kate Lewis, Lisa Maves, and Vicky Prince for providing cDNAs to make in situ probes. The islet, zn5, and 3A10 monoclonal antibodies were obtained from the Developmental Studies Hybridoma Bank developed under the auspices of the NICHD and maintained by The University of Iowa. This work was supported by an NIH training grant fellowship (NIGMS T32 GM08396 to GV) and NIH grants (NS39994 to ROK and NS40449 to AC).

References

Aza-Blanc P, Ramirez-Weber FA, Laget MP, Schwartz C, Kornberg TB. Proteolysis that is inhibited by hedgehog targets Cubitus interruptus protein to the nucleus and converts it to a repressor. Cell 1997;89:1043–1053. [PubMed: 9215627]

Bai CB, Joyner AL. Gli1 can rescue the in vivo function of Gli2. Development 2001;128:5161–5172. [PubMed: 11748151]

Bai CB, Auerbach W, Lee JS, Stephen D, Joyner AL. Gli2, but not Gli1, is required for initial Shh signaling and ectopic activation of the Shh pathway. Development 2002;129:4753–4761. [PubMed: 12361967]

Bai CB, Stephen D, Joyner AL. All mouse ventral spinal cord patterning by hedgehog is Gli dependent and involves an activator function of Gli3. Dev Cell 2004;6:103–115. [PubMed: 14723851]

Barresi MJ, Stickney HL, Devoto SH. The zebrafish slow-muscle-omitted gene product is required for hedgehog signal transduction and the development of slow muscle identity. Development 2000;127:2189–2199. [PubMed: 10769242]

Barth KA, Wilson SW. Expression of zebrafish nk2.2 is influenced by *sonic hedgehog/vertebrate hedgehog-1* and demarcates a zone of neuronal differentiation in the embryonic forebrain. Development 1995;121:1755–1768. [PubMed: 7600991]

Begemann G, Marx M, Mebus K, Meyer A, Bastmeyer M. Beyond the neckless phenotype: influence of reduced retinoic acid signaling on motor neuron development in the zebrafish hindbrain. Dev Biol 2004;271:119–129. [PubMed: 15196955]

Bingham S, Nasevicius A, Ekker SC, Chandrasekhar A. Sonic hedgehog and tiggy-winkle hedgehog cooperatively induce zebrafish branchiomotor neurons. Genesis 2001;30:170–174. [PubMed: 11477700]

Bingham S, Higashijima S, Okamoto H, Chandrasekhar A. The zebrafish trilobite gene is essential for tangential migration of branchiomotor neurons. Dev Biol 2002;242:149–160. [PubMed: 11820812]

Bingham S, Chaudhari S, Vanderlaan G, Itoh M, Chitnis A, Chandrasekhar A. Neurogenic phenotype of mind bomb mutants leads to severe patterning defects in the zebrafish hindbrain. Dev Dyn 2003;228:451–463. [PubMed: 14579383]

Brand M, Heisenberg CP, Warga RM, Pelegri F, Karlstrom RO, Beuchle D, Picker A, Jiang YJ, Furutani-Seiki M, van Eeden FJ, Granato M, Haffter P, Hammerschmidt M, Kane DA, Kelsh RN, Mullins MC, Odenthal J, Nusslein-Volhard C. Mutations affecting development of the midline and general body shape during zebrafish embryogenesis. Development 1996;123:129–142. [PubMed: 9007235]

Chandrasekhar A. Turning heads: development of vertebrate branchiomotor neurons. Dev Dyn 2004;229:143–161. [PubMed: 14699587]

Chandrasekhar A, Moens CB, Warren JT Jr, Kimmel CB, Kuwada JY. Development of branchiomotor neurons in zebrafish. Development 1997;124:2633–2644. [PubMed: 9217005]

Chandrasekhar A, Warren JT Jr, Takahashi K, Schauerte HE, van Eeden FJM, Haffter P, Kuwada JY. Role of sonic hedgehog in branchiomotor neuron induction in zebrafish. Mech Dev 1998;76:101–115. [PubMed: 9767138]

Chandrasekhar A, Schauerte HE, Haffter P, Kuwada JY. The zebrafish *detour* gene is essential for cranial but not spinal motor neuron induction. Development 1999;126:2727–2737. [PubMed: 10331983]

Chen W, Burgess S, Hopkins N. Analysis of the zebrafish smoothened mutant reveals conserved and divergent functions of hedgehog activity. Development 2001;128:2385–2396. [PubMed: 11493557]

Concordet JP, Lewis KE, Moore JW, Goodrich LV, Johnson RL, Scott MP, Ingham PW. Spatial regulation of a zebrafish *patched* homologue reflects the roles of sonic hedgehog and protein kinase A in neural tube and somite patterning. Development 1996;122:2835–2846. [PubMed: 8787757]

Ding Q, Motoyama J, Gasca S, Mo R, Sasaki H, Rossant J, Hui CC. Diminished Sonic hedgehog signaling and lack of floor plate differentiation in Gli2 mutant mice. Development 1998;125:2533–2543. [PubMed: 9636069]

Eisen JS. Motoneuronal development in the embryonic zebrafish. Development 1991;2:141–147. [PubMed: 1842352]

Hatta K. Role of the floor plate in axonal patterning in the zebrafish CNS. Neuron 1992;9:629–642. [PubMed: 1382472]

Higashijima S, Hotta Y, Okamoto H. Visualization of cranial motor neurons in live transgenic zebrafish expressing green fluorescent protein under the control of the islet-1 promoter/enhancer. J Neurosci 2000;20:206–218. [PubMed: 10627598]

Ingham PW, McMahon AP. Hedgehog signaling in animal development: paradigms and principles. Genes Dev 2001;15:3059–3087. [PubMed: 11731473]

Karlstrom RO, Trowe T, Klostermann S, Baier H, Brand M, Crawford AD, Grunewald B, Haffter P, Hoffmann H, Meyer SU, Muller BK, Richter S, van Eeden FJ, Nusslein-Volhard C, Bonhoeffer F. Zebrafish mutations affecting retinotectal axon pathfinding. Development 1996;123:427–438. [PubMed: 9007260]

Karlstrom RO, Talbot WS, Schier AF. Comparative synteny cloning of zebrafish you-too: mutations in the Hedgehog target gli2 affect ventral forebrain patterning. Genes Dev 1999;13:388–393. [PubMed: 10049354]

Karlstrom RO, Tyurina OV, Kawakami A, Nishioka N, Talbot WS, Sasaki H, Schier AF. Genetic analysis of zebrafish gli1 and gli2 reveals divergent requirements for gli genes in vertebrate development. Development 2003;130:1549–1564. [PubMed: 12620981]

Kimmel, CB.; Westerfield, M. Primary neurons of the zebrafish. In: Edelman, GM.; Cowan, WM., editors. Signals and Sense: Local and Global Order in Perceptual Maps. Wiley Interscience; New York: 1990. p. 561-588.

Korzh V, Edlund T, Thor S. Zebrafish primary neurons initiate expression of the LIM homeodomain protein Isl-1 at the end of gastrulation. Development 1993;118:417–425. [PubMed: 8223269]

Krishnan V, Pereira FA, Qiu Y, Chen CH, Beachy PA, Tsai SY, Tsai MJ. Mediation of Sonic hedgehog-induced expression of COUP-TFII by a protein phosphatase. Science 1997;278:1947–1950. [PubMed: 9395397]

Lauderdale JD, Davis NM, Kuwada JY. Axon tracts correlate with *netrin-1a* expression in the zebrafish embryo. Mol Cell Neurosci 1997;9:293–313. [PubMed: 9268507]

Lei Q, Zelman AK, Kuang E, Li S, Matise MP. Induction of graded hedgehog signaling by a combination of Gli2 and Gli3 activator functions in the developing spinal cord. Development 2004;131:3593–3604. [PubMed: 15215207]

Linville A, Gumusaneli E, Chandraratna RA, Schilling TF. Independent roles for retinoic acid in segmentation and neuronal differentiation in the zebrafish hindbrain. Dev Biol 2004;270:186–199. [PubMed: 15136149]

Litingtung Y, Chiang C. Specification of ventral neuron types is mediated by an antagonistic interaction between Shh and Gli3. Nat Neurosci 2000;3:979–985. [PubMed: 11017169]

Lum L, Beachy PA. The Hedgehog response network: sensors, switches, and routers. Science 2004;304:1755–1759. [PubMed: 15205520]

Matise MP, Epstein DJ, Park HL, Platt KA, Joyner AL. Gli2 is required for induction of floor plate and adjacent cells, but not most ventral neurons in the mouse central nervous system. Development 1998;125:2759–2770. [PubMed: 9655799]

Maves L, Jackman W, Kimmel CB. FGF3 and FGF8 mediate a rhombomere 4 signaling activity in the zebrafish hindbrain. Development 2002;129:3825–3837. [PubMed: 12135921]

Mendelson B. Development of reticulospinal neurons of the zebrafish: I. Time of origin. J Comp Neurol 1986;251:160–171. [PubMed: 3782496]

Motoyama J, Milenkovic L, Iwama M, Shikata Y, Scott MP, Hui CC. Differential requirement for Gli2 and Gli3 in ventral neural cell fate specification. Dev Biol 2003;259:150–161. [PubMed: 12812795]

Novitch BG, Wichterle H, Jessell TM, Sockanathan S. A requirement for retinoic acid-mediated transcriptional activation in ventral neural patterning and motor neuron specification. Neuron 2003;40:81–95. [PubMed: 14527435]

Oxtoby E, Jowett T. Cloning of the zebrafish krox-20 gene (krx-20) and its expression during hindbrain development. Nucleic Acids Res 1993;21:1087–1095. [PubMed: 8464695]

Park HL, Bai C, Platt KA, Matise MP, Beeghly A, Hui C, Nakashima M, Joyner AL. Mouse gli1 mutants are viable but have defects in SHH signaling in combination with a gli2 mutation. Development 2000;127:1593–1605. [PubMed: 10725236]

Park HC, Mehta A, Richardson JS, Appel B. olig2 is required for zebrafish primary motor neuron and oligodendrocyte development. Dev Biol 2002;248:356–368. [PubMed: 12167410]

Park HC, Shin J, Appel B. Spatial and temporal regulation of ventral spinal cord precursor specification by Hedgehog signaling. Development 2004;131:5959–5969. [PubMed: 15539490]

Persson M, Stamataki D, te Welscher P, Andersson E, Bose J, Ruther U, Ericson J, Briscoe J. Dorsal–ventral patterning of the spinal cord requires Gli3 transcriptional repressor activity. Genes Dev 2002;16:2865–2878. [PubMed: 12435629]

Prince VE, Joly L, Ekker M, Ho RK. Zebrafish hox genes: genomic organization and modified colinear expression patterns in the trunk. Development 1998;125:407–420. [PubMed: 9425136]

Ruiz i Altaba A. Combinatorial Gli gene function in floor plate and neuronal inductions by Sonic hedgehog. Development 1998;125:2203–2212. [PubMed: 9584120]

Shirasaki R, Pfaff SL. Transcriptional codes and the control of neuronal identity. Annu Rev Neurosci 2002;25:251–281. [PubMed: 12052910]

Stamataki D, Ulloa F, Tsoni SV, Mynett A, Briscoe J. A gradient of Gli activity mediates graded Sonic Hedgehog signaling in the neural tube. Genes Dev 2005;19:626–641. [PubMed: 15741323]

Taipale J, Chen JK, Cooper MK, Wang B, Mann RK, Milenkovic L, Scott MP, Beachy PA. Effects of oncogenic mutations in Smoothened and Patched can be reversed by cyclopamine. Nature 2000;406:1005–1009. [PubMed: 10984056]

Trevarrow B, Marks DL, Kimmel CB. Organization of hindbrain segments in the zebrafish embryo. Neuron 1990;4:669–679. [PubMed: 2344406]

Tyurina OV, Guner B, Popova E, Feng J, Schier AF, Kohtz JD, Karlstrom RO. Zebrafish Gli3 functions as both an activator and a repressor in Hedgehog signaling. Dev Biol 2005;277:537–556. [PubMed: 15617692]

Ungar AR, Moon RT. Inhibition of protein kinase A phenocopies ectopic expression of *hedgehog* in the CNS of wild-type and *cyclops* mutant embryos. Dev Biol 1996;178:186–191. [PubMed: 8812120]

van Eeden FJ, Granato M, Schach U, Brand M, Furutani-Seiki M, Haffter P, Hammerschmidt M, Heisenberg CP, Jiang YJ, Kane DA, Kelsh RN, Mullins MC, Odenthal J, Warga RM, Allende ML, Weinberg ES, Nusslein-Volhard C. Mutations affecting somite formation and patterning in the zebrafish, *Danio rerio*. Development 1996;123:153–164. [PubMed: 9007237]

Varga ZM, Amores A, Lewis KE, Yan YL, Postlethwait JH, Eisen JS, Westerfield M. Zebrafish smoothened functions in ventral neural tube specification and axon tract formation. Development 2001;128:3497–3509. [PubMed: 11566855]

Wechsler-Reya R, Scott MP. The developmental biology of brain tumors. Annu Rev Neurosci 2001;24:385–428. [PubMed: 11283316]

Westerfield, M. The Zebrafish Book. University of Oregon; Eugene, OR: 1995.

Wijgerde M, McMahon JA, Rule M, McMahon AP. A direct requirement for Hedgehog signaling for normal specification of all ventral progenitor domains in the presumptive mammalian spinal cord. Genes Dev 2002;16:2849–2864. [PubMed: 12435628]

Zeller J, Schneider V, Malayaman S, Higashijima S, Okamoto H, Gui J, Lin S, Granato M. Migration of zebrafish spinal motor nerves into the periphery requires multiple myotome-derived cues. Dev Biol 2002;252:241–256. [PubMed: 12482713]

Appendix A. Supplementary Data

Supplementary data associated with this article can be found, in the online version, at doi: 10.1016/j.ydbio.2005.04.010.

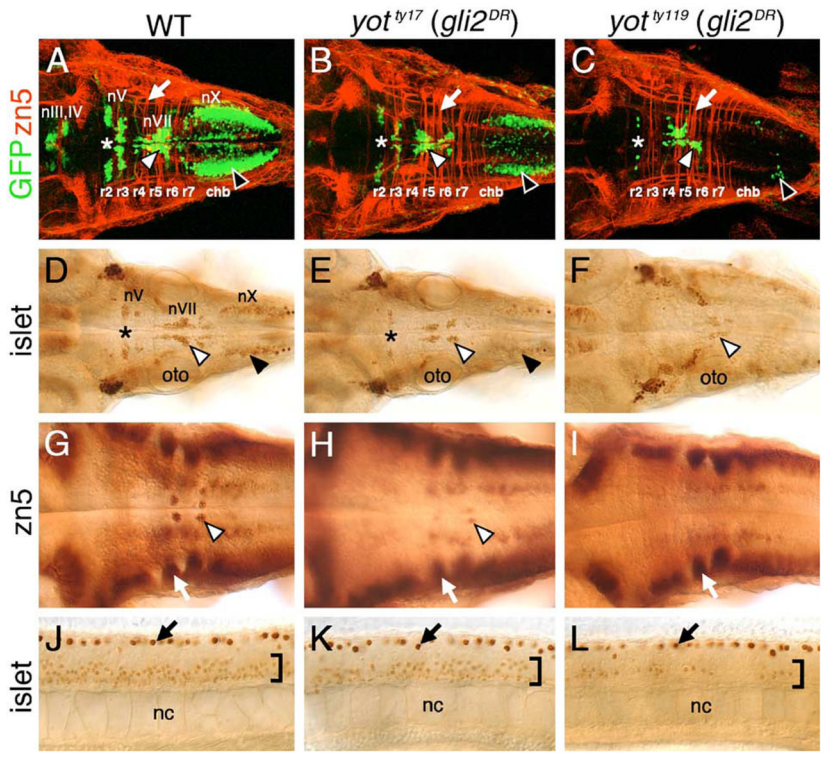

Fig. 1.

Cranial and spinal motor neuron development is affected in *you-too* (*yot*) mutants. Panels A–I show dorsal views of the hindbrain, and panels J–L show lateral views of the trunk, with anterior to the left. Asterisks in A–E indicate the location of nV motor neurons in rhombomere 2. Panels A–C are composite confocal images of embryos and identify *GFP*-expressing cranial motor neurons in the fluorescein channel, and zn5 antibody-labeled commissural neurons and axons at rhombomere boundaries (arrows) in the rhodamine channel. (A–C) In a 48-h post-fertilization (hpf) wild-type embryo (A), the nIII and nIV somatic motor neurons are located in the midbrain, the trigeminal motor neurons (nV; asterisk) in r2 and r3, the facial motor neurons (nVII; white arrowhead) in r5, r6, and r7, and the vagal motor neurons (nX; black arrowhead) in the caudal hindbrain (chb). The nV neurons are reduced in number in *yot*^{ty17} mutants (B), and almost absent in *yot*^{ty119} mutants (C), and, similarly, the nX neurons (black arrowheads) exhibit progressively severe losses in *yot*^{ty17} and *yot*^{ty119} mutants. While nVII neurons (white arrowheads) are also reduced in number in both mutant alleles, the reduction is less severe than those for nV and nX neurons. (D–F) At 36 hpf, the islet antibody labels hindbrain motor neurons in characteristic locations (arrowheads, asterisk; see panel A for details) in wild-type embryos (D), and these neurons are found in progressively reduced numbers in *yot*^{ty17} (E) and *yot*^{ty119} (F) embryos. (G) In a 48-hpf wild-type embryo, the zn5 antibody labels axons and cell bodies of the nVI abducens motor neurons in rhombomeres 5 and 6 (arrowhead), and the commissural neurons at rhombomere boundaries (arrow). (H and I) In both *yot* mutants, the commissural neurons (arrows) develop normally, while the nVI neurons are reduced in number in *yot*^{ty17} mutants (H), and absent in *yot*^{ty119} mutants (I). (J–L) At 36 hpf, the islet antibody labels motor neurons in the ventral spinal cord (bracket) in wild-type embryos (J), and these neurons are found in progressively reduced numbers in *yot*^{ty17} (K) and *yot*^{ty119} (L) embryos. The strongly labeled cells in the dorsal spinal cord (arrows) are Rohon-Beard sensory neurons. oto, otocyst; nc, notochord.

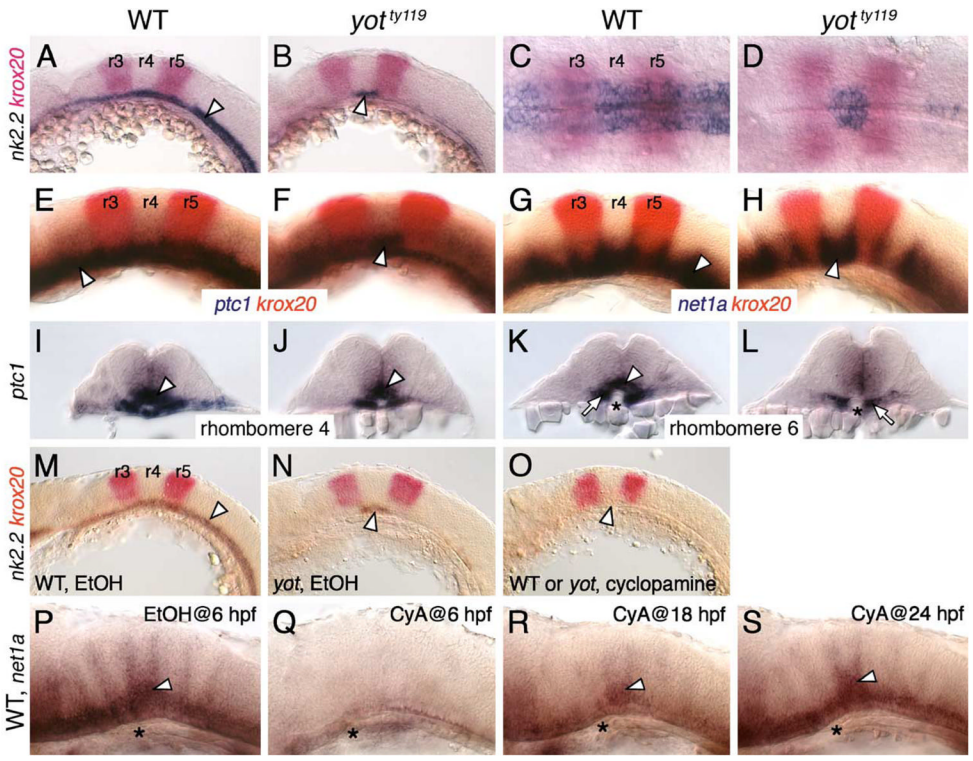

Fig. 2.

Hh signaling is significantly normal in rhombomere 4 of *yot* mutants. Panels A, B, E–H, and M–S show lateral views of hindbrain, with anterior to the left. Panels C and D show dorsal views with anterior to the left. Panels I–L show cross sections of the hindbrain (top is dorsal) at the indicated rhombomere levels. (A–D) In 21 hpf wild-type embryos (A and C), *nk2.2* is expressed (arrowhead) in the ventral neural tube at all axial levels. In yot^{ty119} mutants (B and D), *nk2.2* expression (arrowhead) is virtually absent at all axial levels, except in rhombomere 4 (r4), delineated by the expression of *krox20* in r3 and r5. Within r4 (D), the *nk2.2* expression domain is slightly reduced compared to wild-type. (E–H) In 21 hpf wild-type embryos, *ptc1* (E) and *net1a* (G) are expressed (arrowheads) at all axial levels in the ventral neural tube. In yot^{ty119} mutants, *ptc1* expression (F) is greatly reduced, with significant expression retained in r4 (arrowhead). Similarly, while *net1a* expression is substantially reduced in the yot^{ty119} mutant hindbrain (H), it is significantly normal in r4 (arrowhead). (I–L) In rhombomere 4 (r4), *ptc1* expression (arrowheads) in the ventral neural tube is comparable between wild-type (I) and *yot* mutants (J). In contrast, *ptc1* expression in r6 (K) (arrowhead) is greatly reduced in *yot* mutants (L), while its expression in paraxial mesoderm (arrows) appears normal. Asterisk, notochord. (M–O) While *nk2.2* is specifically expressed in r4 of mutants (N, arrowhead), *nk2.2* expression in all rhombomeres, including r4 (arrowhead), is completely absent in wild-type and mutant embryos treated with cyclopamine (O). (P) In a control 30 hpf wild-type embryo treated with EtOH from 6 hpf, *net1a* expression is normal, with elevated expression in r4 (arrowhead). (Q) In a wild-type embryo treated with cyclopamine (CyA) from 6 hpf, *net1a* expression is completely absent at all axial levels. (R) In an embryo treated from 18 hpf, *net1a* is mostly expressed in r4 (arrowhead). (S) In an embryo treated from 24 hpf, *net1a* expression is mostly normal, with prominent expression in r4 (arrowhead). Asterisks in P–S mark the anterior end of the notochord in r4.

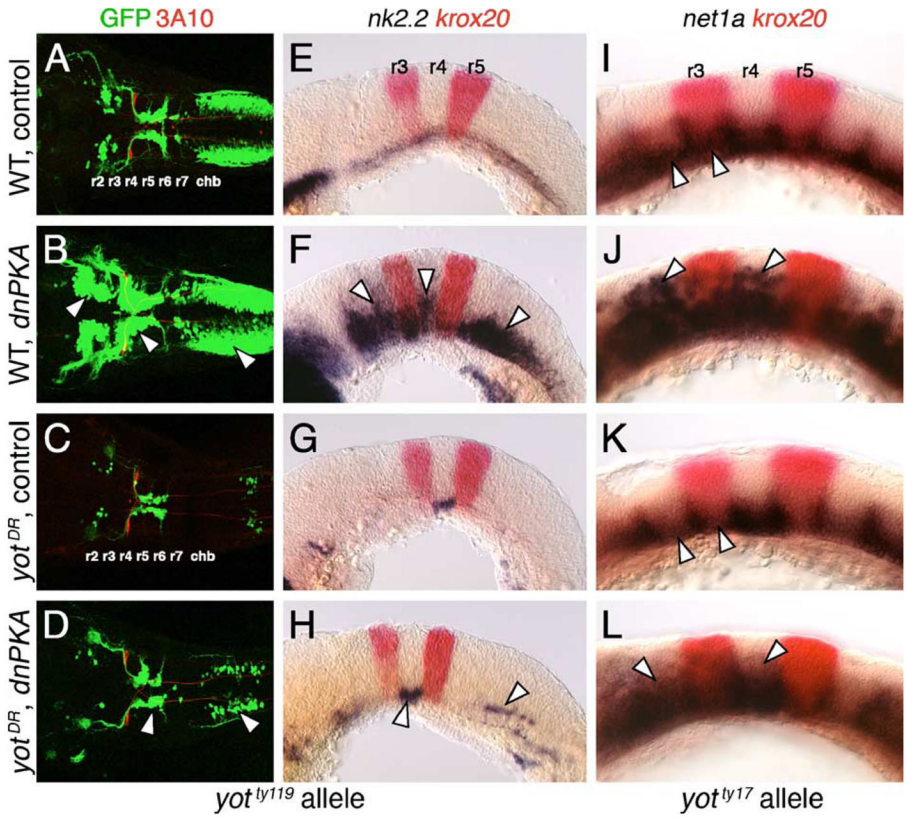

Fig. 3.

Hh-regulated events in *yot*^{ty119} mutants are resistant to ectopic Hh pathway activation. Anterior is to left in all panels. Panels A–D show dorsal views, and panels E–L show lateral views. A–D are composite confocal images of embryos, and identify *GFP*-expressing branchiomotor neurons (green), and 3A10 antibody-labeled Mauthner neurons and axons in rhombomere 4 (red). (A and E) In control wild-type embryos, *nk2.2* is expressed ventrally at all axial levels at 21 hpf (E), and branchiomotor neurons are found at their characteristic locations at 36 hpf (A). (B and F) In *dnPKA* RNA-injected wild-type embryos, *nk2.2* is expressed at high levels, and at ectopic locations (arrowheads) in all rhombomeres (F). Branchiomotor neurons are also greatly increased in number (arrowheads), and found at ectopic locations at all axial levels (B). (C and G) In control *yot*^{ty119} mutants, *nk2.2* expression is missing throughout the hindbrain, except within r4 (G), and, concomitantly, there is a severe loss of branchiomotor neurons at all axial levels, except nVII neurons, which originate in r4 (C). (D and H) In *dnPKA* RNA-injected *yot*^{ty119} mutants, *nk2.2* expression is increased within its normal ventral domain in r4, and slightly within the caudal hindbrain (H, arrowheads). There is a corresponding increase in the number of branchiomotor neurons originating in r4 and the caudal hindbrain (arrowheads), but there is no effect on motor neurons in other rhombomeres (D). (I–L) In a control 21 hpf wild-type embryo (I), *net1a* is expressed ventrally at all axial levels (arrowheads), with dorsal expansion at rhombomere boundaries. In a *dnPKA* RNA-injected wild-type embryo (J), *net1a* expression is expanded dorsally (arrowheads) at all axial levels. In a control *yot*^{ty17} mutant (K), *net1a* expression is reduced in all rhombomeres except r4 (arrowheads; compare to I). In a *dnPKA* RNA-injected *yot*^{ty17} mutant (L), *net1a* expression is expanded dorsally in all rhombomeres including r2 and r4 (arrowheads).

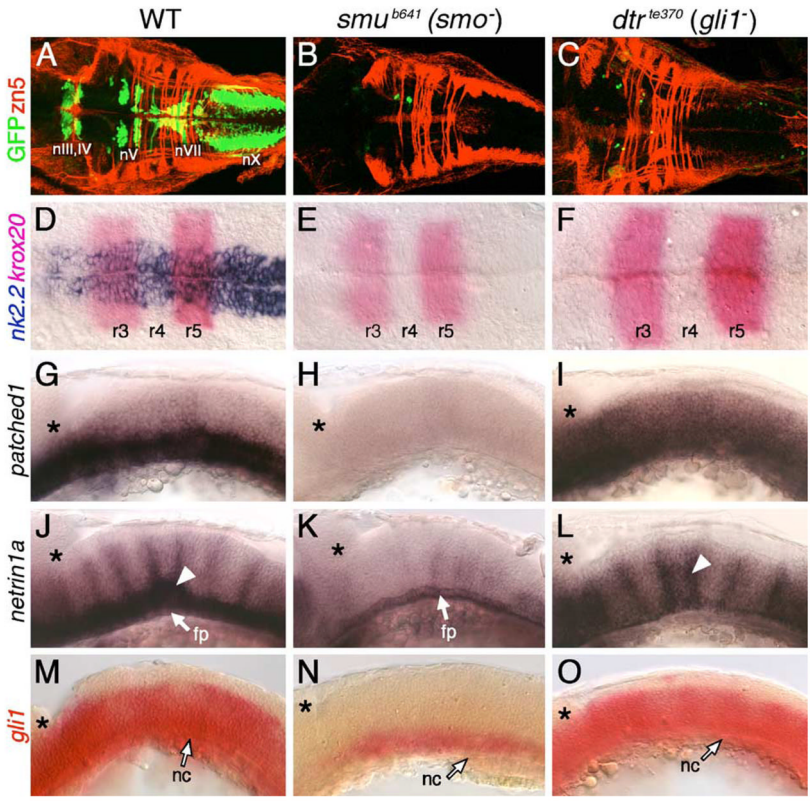

Fig. 4.

Hh signaling and Gli1 function are essential for branchiomotor neuron development. Panels A–F and G–O show dorsal and lateral views, respectively, of the hindbrain with anterior to the left. Asterisks in G–O mark the cerebellum. (A) In a 48-hpf wild-type embryo, the nIII, nIV, nV, nVII, and nX motor neurons are found in their characteristic positions. (B–C) In *slow muscle-omitted* (*smu*; B) and *detour* (*dtr*; C) mutants, *GFP*-expressing cranial motor neurons are almost completely missing, while the zn5-labeled axons at rhombomere boundaries are unaffected. (D) In a 21-hpf wild-type embryo, *nk2.2* is expressed throughout the ventral neural tube at all axial levels. (E–F) In *smu* (E) and *dtr* (F) mutants, *nk2.2* expression is lost, while *krox20* expression in r3 and r5 is unaffected. (G–I) In a 24-hpf wild-type embryo (G), *ptc1* is expressed in the ventral hindbrain, while it is expressed diffusely at a reduced level in *dtr* mutants (I), and not expressed at all in *smu* mutants (H). (J) In a 30-hpf wild-type embryo, *net1a* is expressed in the ventral hindbrain and at rhombomere boundaries (arrowhead). (K) In *smu* mutants, *net1a* expression is mostly lost, with residual expression in the floor plate (fp). (L) In *dtr* mutants, *net1a* expression in the ventral hindbrain is greatly reduced, but expression at rhombomere boundaries (arrowhead) is unaffected. (M–O) In a 21-hpf wild-type embryo (M), *gli1* is expressed in the ventral two-thirds of the neural tube, while its expression is greatly reduced in *smu* mutants (N), and is unaffected in *dtr* mutants (O). The anterior tip of the notochord (nc) is at the level of r4, and is indicated by arrows.

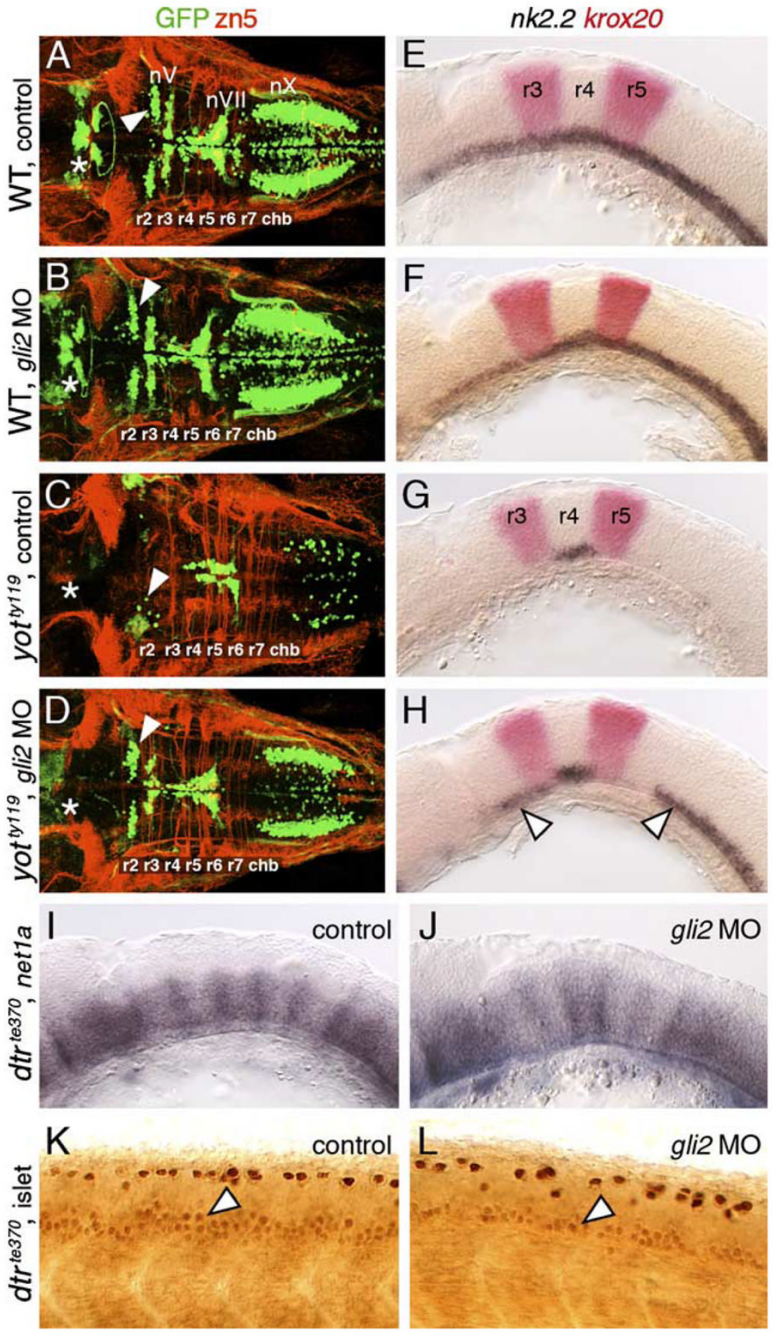

Fig. 5.

Gli2 contributes to spinal motor neuron induction. Panels A–D show dorsal views, and panels E–L show lateral views of the hindbrain (E–J) and spinal cord (K and L), with anterior to the left. Asterisks in A–D indicate the position of the nIII and nIV motor neurons in the midbrain (A and B), and their absence (C and D). Arrowheads in A–D indicate the nV neurons in r2. (A and E) In control wild-type embryos, *nk2.2* expression (E) and organization of cranial motor neurons (A) are identical to those described previously. (B and F) In *gli2* MO-injected wild-type embryos, expression of *nk2.2* (F) and development of cranial motor neurons (B) are identical to control embryos. (C and G) In control yot^{ty119} mutants, the patterns of loss of *nk2.2* expression (G) and cranial motor neurons (C) are similar to those described previously.

(D and H) In *gli2* MO-injected *yot*^{ty119} mutants, *nk2.2* expression is significantly restored in anterior rhombomeres and the caudal hindbrain (H, arrowheads). Concomitantly, the number of nV neurons (arrowhead) and nX neurons is significantly increased (D), and the pattern looks similar to that in control wild-type embryos. (I and K) In control *dtr*^{te370} mutants, *net1a* is expressed at low levels in the ventral hindbrain, and at higher levels at rhombomere boundaries (I). In the mutant spinal cord (K), islet antibody-labeled motor neurons (arrowhead) are found in similar numbers to wild-type embryos. (J and L) In *gli2* MO-injected *dtr*^{te370} mutants, *net1a* expression in the hindbrain (J) shows no significant change (loss). In contrast, the number of motor neurons in the ventral spinal cord (arrowhead) is slightly but reproducibly reduced in MO-injected mutants (L).

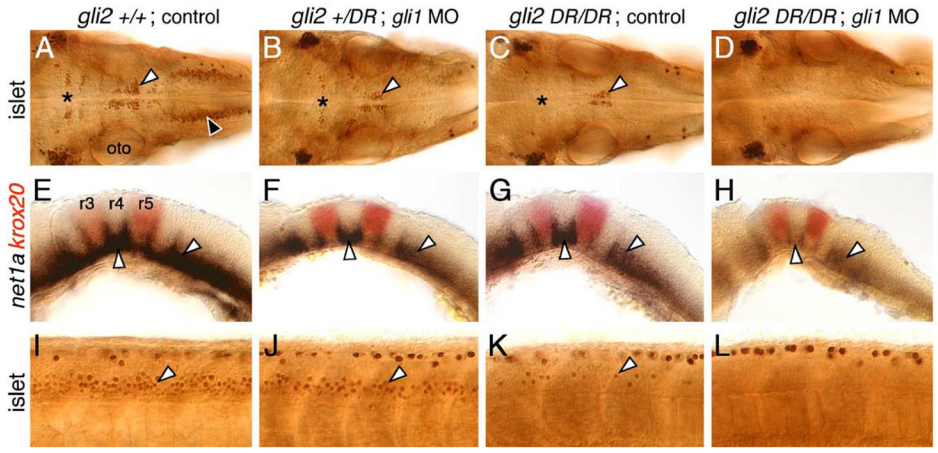

Fig. 6.

Gli1 contributes to spinal motor neuron induction. Panels A–D show dorsal views, and panels E–L show lateral views, with anterior to the left. (A, E, and I) In an uninjected 36 hpf wild-type (*yot*+/+ or +/−) embryo, islet antibody labeling (A) reveals the characteristic organization of the nV neurons in r2 (asterisk), the nVII neurons (white arrowhead), the nX neurons (black arrowhead), and the patterned expression of *net1a* (E) in the ventral hindbrain and at rhombomere boundaries (arrowheads). Spinal motor neurons (arrowhead, I) are found in characteristic numbers. (B, F, and J) In a yot^{ty119}+/− heterozygote injected with *gli1* MO, nV and nVII neurons are reduced in number (asterisk, arrowhead in B), nX neurons are absent, and *net1a* expression is significantly reduced in the hindbrain (arrowheads, F). Spinal motor neurons are slightly reduced in number (arrowhead, J). (C, G, and K) In an uninjected yot^{ty119} mutant, nV (asterisk, C), nX, and spinal motor neurons (arrowhead, K) are greatly reduced in number, while the nVII neurons (arrowhead, C) show a moderate reduction. *Net1a* expression is significantly reduced in the hindbrain (arrowheads, G). (D, H, and L) In a yot^{ty119} mutant injected with *gli1* MO, branchiomotor (D) and spinal motor neurons (L) are completely absent. *Net1a* expression (arrowheads, H) is also severely reduced in the hindbrain. The strongly labeled cells in the dorsal spinal cord (I–L) are Rohon-Beard sensory neurons, which are unaffected by these treatments.

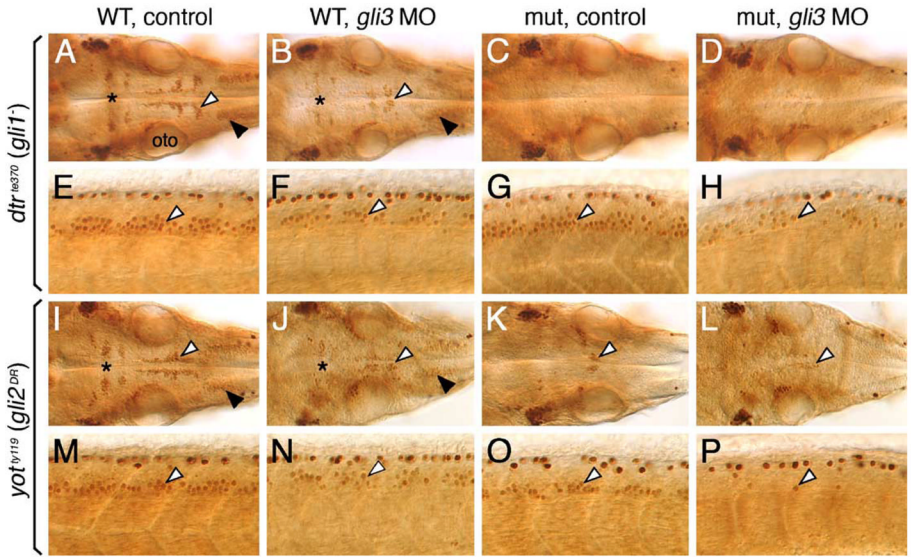

Fig. 7.

Gli3 plays a role in branchiomotor and spinal motor neuron induction. Panels A–D and I–L show dorsal views of the hindbrain, and panels E–H and M–P show lateral views of the spinal cord, with anterior to the left. (A and E) In an uninjected 36 hpf wild-type (*dtr*+/+ or +/−) embryo, islet antibody labeling reveals the characteristic organization of the nV neurons in r2 (asterisk), the nVII neurons (white arrowhead), and the nX neurons (black arrowhead) in the hindbrain (A), and the characteristic distribution of motor neurons (arrowhead, E) in the ventral spinal cord. (B and F) In a wild-type sibling injected with *gli3* MO, the nV (asterisk), nVII (white arrowhead), and nX (black arrowhead) neurons in the hindbrain (B), and spinal motor neurons (arrowhead, F) are reduced in number. (C, D, G, and H) In an uninjected *dtr* mutant (C), branchiomotor neurons are essentially absent, and this phenotype is maintained in a *gli3* MO-injected *dtr* mutant (D). In contrast, spinal motor neurons are moderately reduced in number in a *gli3* MO-injected *dtr* mutant (arrowhead, H) compared to an uninjected *dtr* mutant (arrowhead, G). (I, J, M, and N) In an uninjected wild-type (*yot*+/+ or +/−) embryo, branchiomotor neurons are found in characteristic numbers (I; see A for details), and their numbers are moderately reduced in a *gli3* MO-injected wild-type sibling (J). Similarly, spinal motor neurons are reduced in number in a *gli3* MO-injected wild-type embryo (arrowhead, N) compared to an uninjected wild-type sibling (arrowhead, M). (K, L, O, P) In an uninjected *yot* mutant (K), most branchiomotor neurons, except nVII neurons (arrowhead), are greatly reduced in number or absent, and the number of nVII neurons is slightly decreased in a *gli3* MO-injected *yot* mutant (L). In contrast, spinal motor neurons are greatly reduced in number in a *gli3* MO-injected *yot* mutant (arrowhead, P) compared to an uninjected *yot* mutant (arrowhead, O). oto, otocyst.

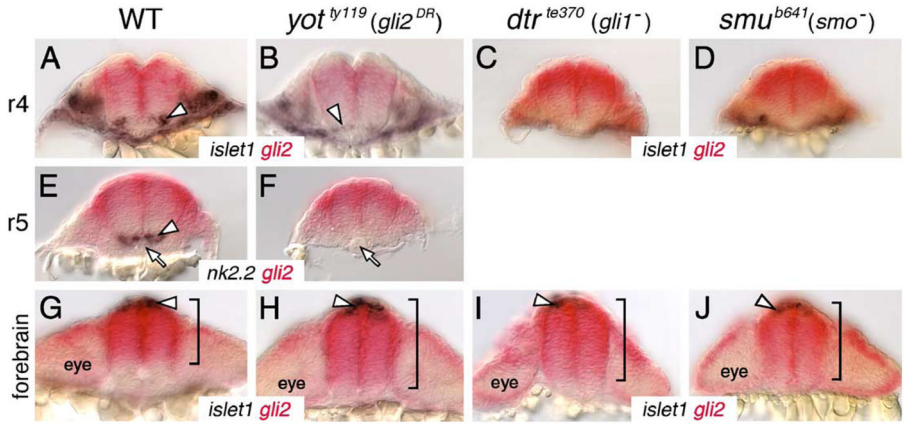

Fig. 8.

Gli2 expression is affected in the forebrain, but not in the hindbrain, of Hh pathway mutants. All panels show cross sections of the neural tube at the indicated axial levels, with dorsal at the top. Embryos were processed for *islet1* (purple); *gli2* (red) (A–D, G–J) or *nk2.2* (purple); *gli2* (red) (E and F) two-color in situs. (A–D) In r4 of a wild-type embryo (A), *islet1*-expressing motor neurons (arrowhead) are located just ventral to the *gli2* expression domain. Similarly, the few *islet1*-expressing neurons in *yot* mutants (arrowhead) are located ventral to the *gli2* expression domain (B), and *gli2* expression does not extend into the ventral-most neural tube in *dtr* (C) and *smu* (D) mutants. (E and F) In r5, while *nk2.2*-expressing cells (arrowhead) are found immediately adjacent to the floor plate and notochord (arrow) in a wild-type embryo (E), *nk2.2* expression is absent in *yot* mutants (F), but the *gli2* expression domain does not expand ventrally. (G–J) At the forebrain level, the *islet1*-expressing epiphysial neurons (arrowhead) are located at the roof of the neural tube. In a 21-hpf wild-type embryo (G), *gli2* expression is limited to the dorsal two-thirds of the neural tube (bracket). In contrast, in yot^{ty119} (H), dtr^{te370} (I), and smu^{b641} (J) mutants, the *gli2* expression domain is expanded ventrally to different extents (brackets).

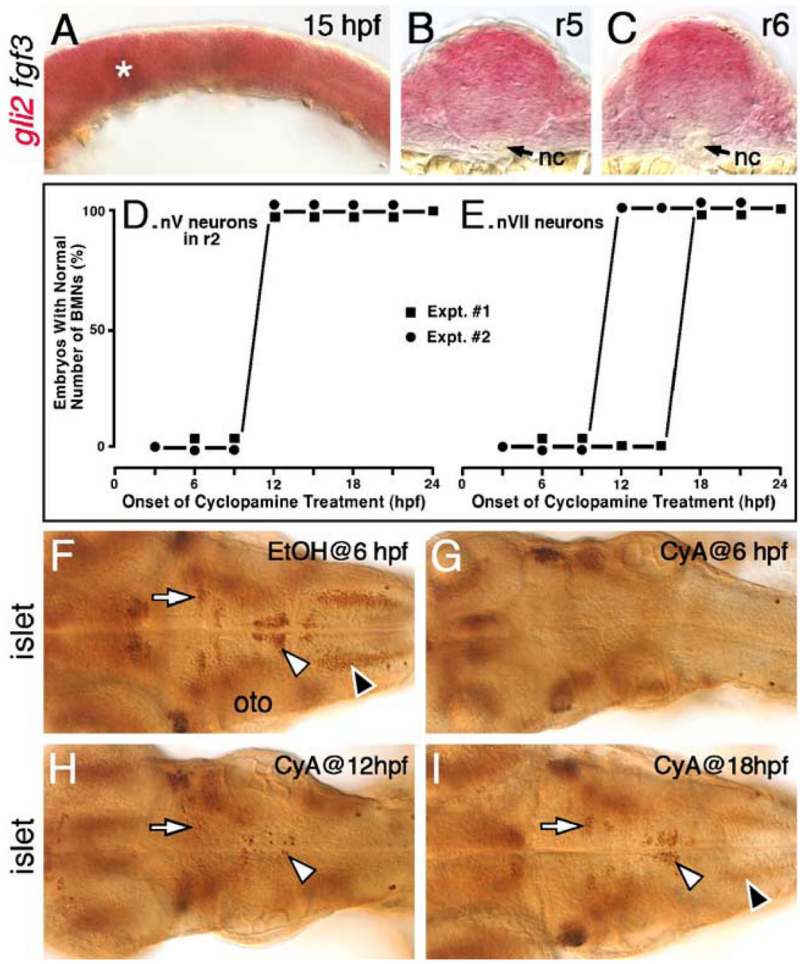

Fig. 9.

Hh signaling is required before 18 hpf for the induction of branchiomotor neurons. Panel A shows a lateral view, and panels F–I show dorsal views of the hindbrain, with anterior to the left. (A) In a 15-hpf wild-type embryo, *gli2* is expressed at all axial levels throughout the dorsoventral extent of the hindbrain. The asterisk marks low level of *fgf3* expression at the mid-hindbrain boundary, which was used to orient embryos for sectioning (see Materials and methods for details). (B and C) Cross-sections (dorsal is up) showing that *gli2* is expressed in the ventral aspects of the neural tube in rhombomeres 5 and 6, but at lower levels than in the dorsal neural tube. nc, notochord. (D and E) Quantification of embryos with normal numbers of *GFP*-expressing nV motor neurons in r2 (D) and nVII neurons in r4–r7 (E) following cyclopamine (CyA) treatment beginning at the times indicated (hpf). There is no effect on nV neuron number in r2 when CyA treatment is initiated at 12 hpf or later (2 experiments; 20 embryos per experiment). There is no effect on nVII neuron number when CyA treatment is initiated at 18 hpf or later (2 experiments). (F) In a 48-hpf wild-type embryo treated with ethanol (EtOH) from 6 hpf, islet antibody labeling reveals that the number and organization of branchiomotor neurons, including nV (arrow), nVII (white arrowhead) and nX (black arrowhead), are unaffected. (G) In an embryo treated with CyA from 6 hpf, islet-labeled branchiomotor neurons are absent. (H) In an embryo treated with CyA from 12 hpf, nV neurons in r2 are mostly present (arrow; light staining), nVII neurons are greatly reduced in number (arrowhead), and nX neurons are absent. (I) In an embryo treated with CyA from 18 hpf, the

nV (arrow), nVII (white arrowhead), and nX neurons (black arrowhead; out of focus) are mostly unaffected. oto, otocyst.

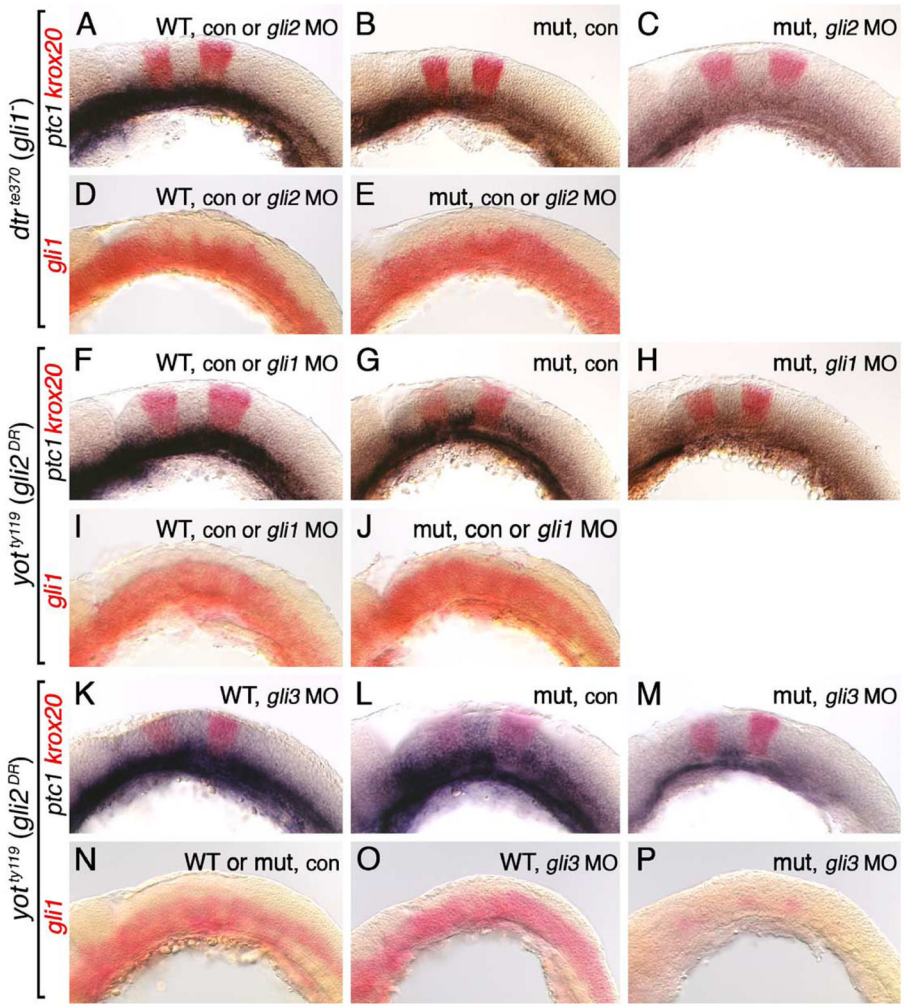

Fig. 10.

Regulation of *gli1* expression requires Gli3, but not Gli1 or Gli2, function. All panels show lateral views of the hindbrain with anterior to the left. Embryos in A–E were obtained from crosses between dtr^{te370}+/− heterozygotes, while those in F–P were obtained from crosses between yot^{ty119}+/− heterozygotes. *Krox20* expression (red) in *ptc1;krox20* double in situ panels identifies rhombomeres 3 and 5. (A) In 21 hpf uninjected or *gli2* MO-injected wild-type embryos, *ptc1* is expressed at all axial levels in the ventral hindbrain. (B) In an uninjected *dtr* mutant, *ptc1* expression is significantly reduced. (C) In a *gli2* MO-injected *dtr* mutant, *ptc1* expression is completely lost in the hindbrain. (D) In a 21-hpf uninjected or *gli2* MO-injected wild-type embryo, *gli1* is expressed at all axial levels in the ventral half/two-thirds of the hindbrain. (E) *Gli1* expression is unaffected in control or *gli2* MO-injected *dtr* mutants. (F–H) *Ptc1* expression is normal in uninjected or *gli1* MO-injected wild-type embryos (F), is reduced significantly in an uninjected *yot* mutant (G), and is completely lost from the hindbrain in a *gli1* MO-injected *yot* mutant (H). (I and J) *Gli1* is expressed normally in the ventral hindbrain in uninjected or *gli1* MO-injected wild-type (I) or *yot* mutants (J). (K–M) *Ptc1* expression is slightly reduced in a *gli3* MO-injected 22 hpf wild-type embryo (K), is reduced significantly in an uninjected 24 hpf *yot* mutant (L), and is almost completely lost in a *gli3* MO-injected 22 hpf *yot* mutant (M). (N–P) *Gli1* is expressed normally in the ventral hindbrain in uninjected wild-type or *yot* mutant embryos (N), and in a *gli3* MO-injected wild-type embryo (O). In a *gli3* MO-injected *yot* mutant, *gli1* expression is greatly reduced (P).

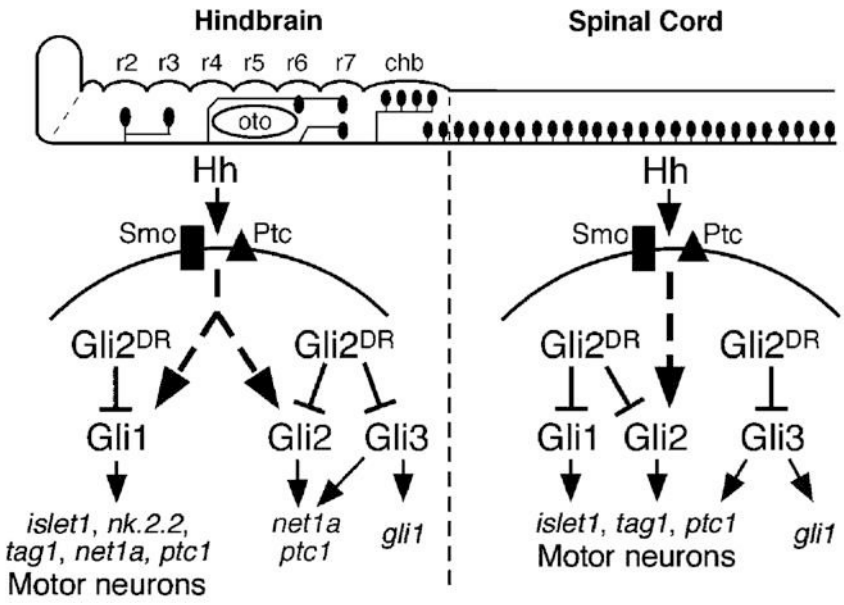

Fig. 11.

Model to explain motor neuron phenotypes of *dtr* (*gli1*$^{-}$) and *yot* (*gli2*^{DR}) mutants, and of *gli1*, *gli2*, and *gli3* morpholino injection experiments. The hindbrain and spinal cord are shown schematically in lateral view (anterior is to left), with the branchiomotor and spinal motor neurons depicted as black ovals. Rhombomeres 2–7 (r2–r7) and the caudal hindbrain (chb) are indicated. The pathways depict signaling within ventral neural tube cells upon transduction of Hh signal through the Smoothened (Smo, black rectangle)-Patched (Ptc, black triangle) receptor system. In the hindbrain, Hh-mediated induction of motor neurons (and motor neuron markers like *nk2.2*, *islet1*, and *tag1*) is completely dependent on *gli1* function. Branchiomotor neuron loss in *yot* mutants appears to result from the action of mutant Gli2 (Gli2^{DR}) on Gli1 activator function. Complete activation of *net1a* and *ptc1* expression requires activator function of Gli1, Gli2, and Gli3. In the spinal cord, Gli1, Gli2, and Gli3 activator functions contribute to spinal motor neuron induction (and *islet1* and *tag1* marker gene expression). The significant loss of spinal motor neurons in *yot* mutants appears to result from the dominant repressor effect of Gli2^{DR} on all Gli activators. *Gli1* expression in the hindbrain and spinal cord appears to specifically require Gli3 activator function.

Table 1

Motor neuron induction is reduced in the hindbrain and spinal cord of *you-too* mutants

Phenotype*	Number of islet antibody-labeled cells		
	Hindbrain (nV, nVI, nVII neurons)#	Hindbrain (nVI, nVII neurons)§	Ventral spinal cord (motor neurons)@
WT (ty17)	201.2 ± 26.4	137.8 ± 18.5	21.8 ± 1.3
you-too^{ty17}	96.5 ± 14.9	72.3 ± 11.4	12.7 ± 4.0
Ratio (mut/WT)	0.48	0.53	0.58
Wt (ty119)	190.3 ± 24.9	132.3 ± 16.9	23.1 ± 1.4
you-too^{ty119}	45.3 ± 6.5	42.8 ± 7.2	4.8 ± 0.8
Ratio (mut/WT)	0.24	0.32	0.21

* Six embryos were scored for each phenotype.

\# Total number of labeled cells in rhombomeres 2–7.

§ Total number of labeled cells in r4–r7 (nVI and nVII neurons in WT, nVII neurons in mutants).

@ Number of labeled cells per hemisegment.

Table 2

Effects of ectopic Hh pathway activation on hindbrain gene expression in *yot* mutants

***yot* allele (marker gene)**	**Injected RNA**	**Number of Embryos**	**Fraction of embryos with ectopic marker expression**	
			Wild-type (+/+ and +/−)[#]	**Mutant (−/−)[#]**
you-too^{ty17}(*netrin1a* expression at21 hpf)	none	137	0% (0/97)	0% (0/40)
	dnPKA[*]	128	91% (84/92)	81% (29/36)
you-too^{ty119}(*nk2.2* expression at21 hpf)	none	32	0% (20/20)	0% (12/12)
	dnPKA[*]	60	88% (38/43)	0% (0/17)[@]
you-too^{ty119} (*islet1-GFP* expression at36 hpf)	none	27	0% (20/20)	0% (7/7)
	dnPKA[*]	52	79% (30/38)	0% (0/14)[@]

[#]While *dnPKA*- injected *yot* mutants could be readily identified after in situ hybridization, roughly half of the embryos in each experiment was genotyped by PCR. Since there was perfect correlation between PCR genotyping and morphological identification, the data from embryos scored by the two methods were pooled.

[*]Approximately 1 ng of *dnPKA* RNA (see Materials and methods) was injected per embryo, generating the Hh overexpression phenotype in 80–90% of injected wild-type embryos (Chandrasekhar et al., 1999).

[@]Although no *nk2.2*-or *GFP*- expressing cells were found at ectopic locations in the *yot*^{ty119} mutant hindbrain following *dnPKA* overexpression, expressing cells were found in the caudal hindbrain of several embryos, where nX neurons are normally found (see Figs. 3D, H). In addition, the number of *GFP*-expressing nVII neurons was markedly increased, and *nk2.2* expression in ventral r4 was consistently upregulated in many of these embryos.

Table 3

Gli2 and *Gli3* contribute to spinal motor neuron induction[@]

Morpholino	Number of islet-labeled cells in the hindbrain		Number of islet-labeled cells in ventral spinal cord[#]	
	Wild-type (*gli1*+)[*]	*dtr* mutant (*gli1*−/−)[*]	Wild-type (*gli1*+)[*]	*dtr* mutant (*gli1*−/−)[*]
none	294.8 ± 14.6 (6)	16.7 ± 10 (6)	22.3 ± 2.3 (6)	20.4 ± 0.6 (6)
gli2 MO[§]	294 ± 25.4 (6)	5.2 ± 2.8 (6)	22.7 ± 2.1 (6)	15.6 ± 1.2 (6)
	$P > 0.05$ (NS)	$P > 0.05$ (NS)	$P > 0.05$ (NS)	$P < 0.001$
none	287.5 ± 22 (4)	12 ± 4.5 (4)	35.2 ± 3.4 (4)	38.9 ± 4.5 (4)
gli3 MO[£]	214.5 ± 5.3 (4)	14.8 ± 3.3 (4)	16.2 ± 2.6 (4)	13.6 ± 2.9 (4)
	$P < 0.001$	$P > 0.05$ (NS)	$P < 0.001$	$P < 0.001$

[@]While the numbers of control and MO-injected embryos were much higher (>40 for each treatment), we counted motor neuron cell bodies in 4–6 representative embryos for each condition. Mutant embryos were identified by the severe loss of hindbrain motor neurons.

[#]Number of labeled cells per hemisegment.

[*]Number of embryos scored in parenthesis.

[§]Approximately 10 ng of *gli2* MO (see Materials and methods) was injected per embryo based upon previous studies (Karlstrom et al., 2003).

[£]Approximately 30 ng of *gli3* MO was injected per embryo. In our hands, this high dose was needed to generate the ectopic *fkd4* expression phenotype described for *gli3* morphants (Tyurina et al., 2005). No non-specific effects were seen, and >90% of injected embryos survived and were healthy when fixed at 36 hpf.

Table 4

Gli2^{DR} interferes with Gli1 and Gli3 activator functions[@]

Morpholino	Number of islet-labeled cells in the hindbrain		Number of islet-labeled cells in ventral spinal cord[#]	
	WT heterozygotes (*gli2*+/DR)[*]	*yot* mutant (*gli2* DR/DR)[*]	WT heterozygotes (*gli2*+/DR)[*]	*yot* mutant (*gli2* DR/DR)[*]
none[§]	223 ± 5 (4)	56.5 ± 4.4 (4)	34 ± 2.9 (4)	4.2 ± 1.4 (4)
gli1 MO[£]	93.8 ± 8.2 (4)	2.3 ± 2.1 (4)	25.9 ± 5.8 (4)	0.5 ± 0.1 (4)
	$P < 0.001$	$P < 0.001$	$P < 0.01$	$P < 0.05$
none[§]	304.8 ± 23.6 (5)	84.6 ± 22.9 (5)	33.6 ± 2.2 (5)	19.4 ± 0.7 (5)
gli3 MO[†]	233 ± 33.2 (5)	118.8 ± 32.1 (5)	16.4 ± 2.1 (5)	3.1 ± 1.7 (5)
	$P < 0.01$	$P > 0.05$ (NS)	$P < 0.001$	$P < 0.001$

[@]While the numbers of control and MO-injected embryos were much higher (>40 for each treatment), we counted motor neuron cell bodies in 4–5 representative embryos for each condition. Embryos were genotyped by PCR.

[#]Number of labeled cells per hemisegment.

[*]Number of embryos scored in parenthesis.

[£]Approximately 5 ng of *gli1* morpholino (see Materials and methods) was injected per embryo. In our hands, this amount did not result in an observable loss of *nk2.2* expression in wild-type embryos as described previously (Karlstrom et al., 2003), suggesting that it is a suboptimal dose. Injection of larger doses generated deformed embryos, and was not pursued further.

[§]The numbers of hindbrain and spinal motor neurons in control wild-type and mutant embryos in the two experiments (performed about one year apart) are substantially different. We attribute these differences to variations in age of embryos, islet antibody staining intensity, and genetic background. Importantly however, the responses to *gli1* and *gli3* MO injections are very similar between the two experiments.

[†]Approximately 30 ng of *gli3* MO was injected per embryo. See Table 3 for details.

Table 5

Ventral expansion of *gli2* expression domain in the forebrain of Hh pathway mutants

Gene	Ventral margin of *gli2* expression domain[#]		*P*
	Wild-type[*]	Mutant[*]	
smu^{b641}	63 ± 8% (5s, 5e)	92 ± 8% (2s, 2e)	< 0.02
dtr^{te370}	63 ± 9% (4s, 4e)	74 ± 1% (7s, 5e)	< 0.005
yot^{ty119}	68 ± 5% (6s, 5e)	83 ± 5% (5s, 5e)	< 0.001

[#] Forebrain sections were scored at the level of the epiphysis, which was identified by the presence of *islet1*-expressing cells (Figs. 8G–J). The dorsoventral height of the neural tube was measured, and the length of the *gli2* expression domain (measured from the dorsal surface) was expressed as a fraction (%) of the height of the neural tube.

[*] The first number in the parenthesis indicates the total number of sections scored, while the second number indicates the number of embryos these sections came from.